Senior Design Program
Mechanical & Aerospace Engineering ▪ The University of Texas at Arlington

Fall 2019 Senior Design Presentations – Friday, May 3rd 1 PM

The Mechanical & Aerospace Engineering Department cordially invites all students, faculty, staff and friends to come hear our Senior Design teams make their final project presentations. Join us to learn about their innovative work in areas as diverse as assistive robotics, factory automation, and electric scooters. Attend just one presentation, or stay the whole time on **Friday, May 3rd** from **1 to 5 pm** in **Nedderman Hall 105**.

1:00	***Airbus Engine Intake*** Cool-Aero, LLC	***15 MINUTE BREAK***	**3:00**	***Variable Displacement Combustion Engine*** Kinetic Consulting, Inc.
1:15	***Airbus Inlet Barrier Filter System*** Edetech, Inc.		**3:15**	***ASHRAE Student Design Competition*** Summit Global Air Solutions, Inc.
1:30	***Integrated In-Wheel Motor Design*** Nextgen Drive, Inc.		**3:30**	***Enhanced Preform Knitter*** Maverick Manufacturing
1:45	***Electric Scooter*** Cage Consulting Co.		**3:45**	***Convolution Spindle*** Tube Dudes
2:00	***3D Printed Aircraft Wing*** Forward Air, LLC		**4:00**	***Carbon Monocoque*** CM Engineering
2:15	***3D Printed Aircraft Fuselage*** 3DAF, Inc.		**4:15**	***Wheelchair Dynamometer*** Gryphon Design Co.
2:30	***Wheelchair Attachable Assistive Arm*** Assistive Robotic Machines, Inc.			

University of Texas Arlington

The UTA ME Senior Design Program would like to extend a grateful acknowledgment to the corporations, faculty, and individuals that in so many ways support and enable the accomplishments of our senior engineering class. Their generous contribution of resources, time and expertise make the difference between just completing an academic requirement, and having a great, enduring learning experience in real-life engineering.

The following entities and individual sponsors contributed direct financial or in-kind support to our student teams:

- Airbus Helicopter, Grand Prairie, Texas.
- Parker Hannifin, Fort Worth, Texas.
- Stratasys, Ltd., Eden Prairie, Minnesota.
- AmeriBand LLC – Dr. Robert Knezek, Arlington, Texas.
- ASHRAE Fort Worth Chapter, Dallas, Texas.
- UTA College of Nursing & Health Innovation, Arlington, Texas.
- UTA Racing, Arlington, Texas.

We acknowledge the dedication, able support and direction of our faculty advisors Profs. Bob Woods, Robert Taylor, Panos Shiakolas, Yawen Wang, and Raul Fernandez.

We gratefully acknowledge the professional support provided by our Machine Shop (Messrs. Kermit Beird and Sam Williams), and Graduate Teaching Assistant (Mr. Joakim Lea).

We very gratefully acknowledge our invited speakers for the Senior Design Lecture Series— Messrs. Alford, Perkowski, Sommerman and Paramo, and Ms. Dickens, as well as all unnamed individuals, including several faculty in the Colleges of Engineering, Science, and Nursing & Health Innovation that help our students with questions and sharing of lab resources. We hope you enjoy these presentations.

Sincerely,
Raul Fernandez

UNIVERSITY OF TEXAS ARLINGTON

VENUE & PARKING INFORMATION

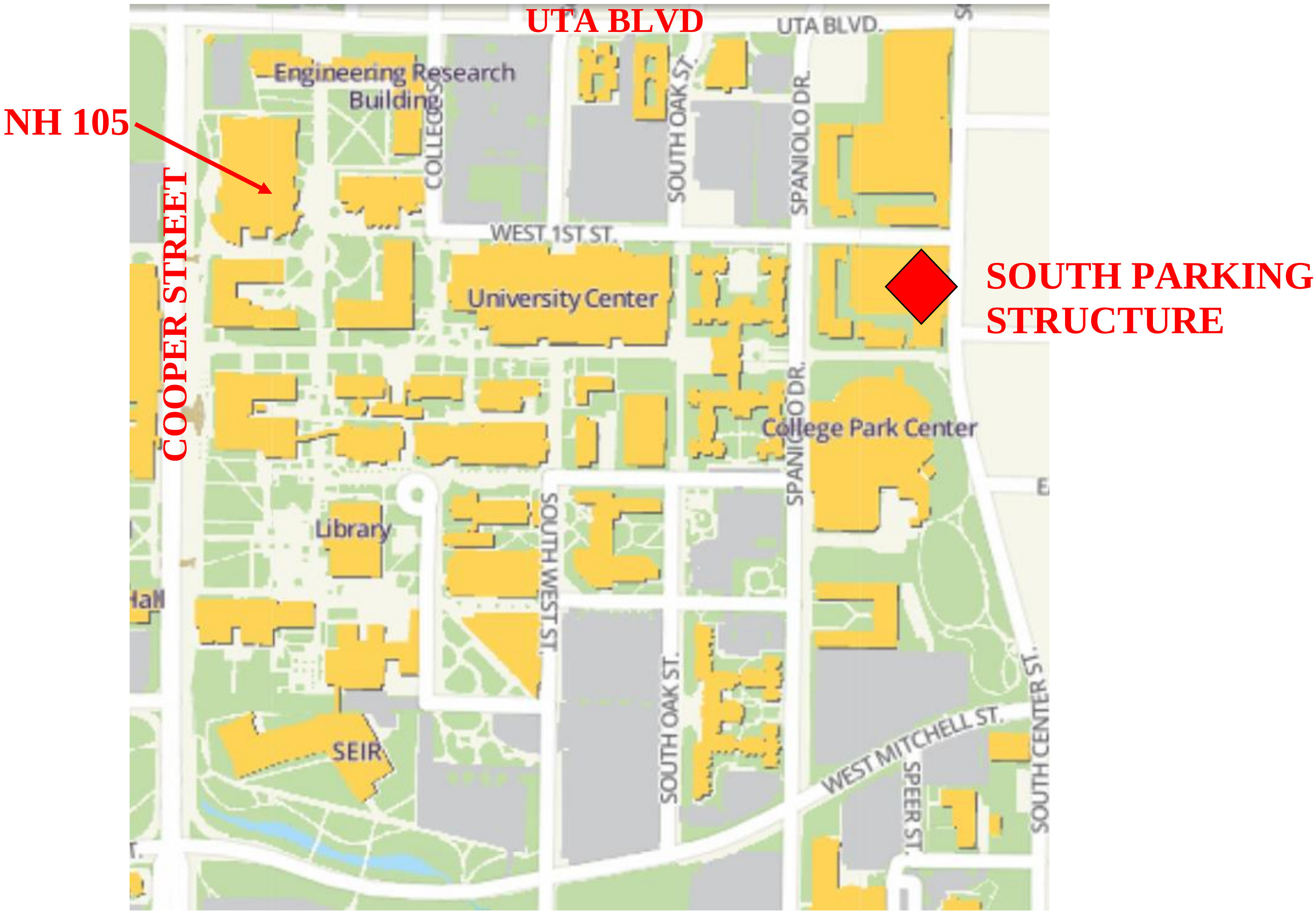

UNIVERSITY OF TEXAS ARLINGTON

SENIOR DESIGN TEAM PHOTOS

CoolAero Industries

COOL-AERO

Alexander Murillo *Team/CFD Lead*
Manuel Tovar *CFD Lead*
Abram Mendez *CAD Lead*
David Allen *Data Lead*

EDETECH

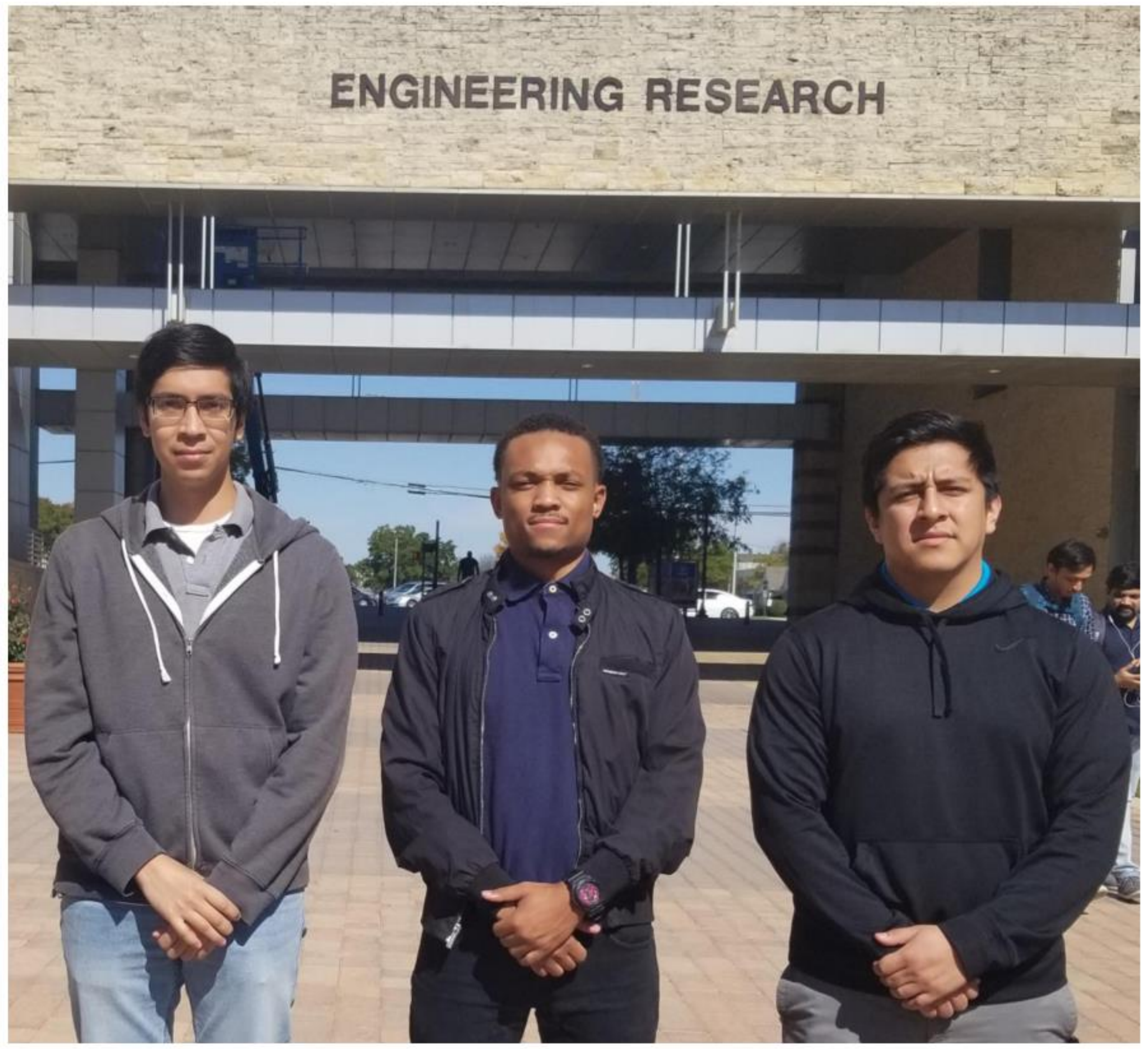

Edgar Cervantes Research & Data Lead
Dante Seay CAD & Experimental Lead
Elias Mata Team & Design Lead

NextGen Drive

NGD NEXTGEN DRIVE

Logan Pechal Manufacturing Strategist
Jacob Lamotte-Dawaghreh Analysis Lead
Matthew Smith Design Lead
Joseph Herring IPT Lead
Garrett Tolar Prototype Strategist
Tim Pugliese Research Lead

Cage Consulting

CAGE CONSULTING

Matt Woods *Research*
Nick Navarette *ANSYS / Stress*
Alex Garcia *Solid Modeling*
Cooper Rush *Solid Modeling*
Jeremy Smith *Team Lead*
Travis Malke *Solid Modeling*

SENIOR DESIGN TEAM PHOTOS

Forward Air

Matthew Montoro, Kaushik Iyer, Salah Abusalah, Traevis Joshlin, Noor Diya, Bosah Agoula, Zeshan Ahmed

3DAF

Bijan Niakan *Team Lead/ Optimization*
April Horton *Optimization*
Ethan Scarlett *CAD Design*
Shibo Yu *CAD Design*
Veronica Harmina *3D Printing*
Abraham Jimenez *3D Printing*

Assistive Robotic Machines

Jeremy Trollinger *CAD Lead*
Lorenzo Alba *Documentation Lead*
Amelia Jackson *Team Lead*
Michaela Stallings *Technical Lead*
Collin Chapin *Stress Analysis Lead*
Regan Kubicek *Research Lead*

Kinetic Konsulting

Erica Glidewell *Systems Engineer*
Robert Goller *Lead Engineer*
Jonathan Fredrickson *Quality Engineer*
Travis Riley *Design Engineer*
Michael Paradis *Design Engineer*
Peter Hymel *Systems Engineer*

SENIOR DESIGN TEAM PHOTOS

Summit Group

Summit Global Air Solutions

Jose Andino *Equipment Specialist Lead*; **Everardo Soto** *Research Lead*; **Saroj Sapkota** *Cad Lead*; **Ang Dorje Sherpa** *Technical Information Lead*; **Bryan Cornell** *Team Lead*

Maverick Manufacturing

Jarrod Rowlette *Materials Science Engineer*; **Andrew Hong** *Manufacturing Engineer*; **Marc Garcia** *Project Manager*; **Thong Nguyen** *Project Engineer*; **Thien Tran** *CAD Engineer*; **Blake Anderson** *CAD Engineer*

TubeDudes

Mihirkumar Patel; La'Varris Carter; Will McKenna; Carter Brown; William Anthony

CM Engineering

CM Engineering

Taylor Shead *CAD Lead*; **Jeff Miller** *Project Engineer*; **Andrew Cardamone** *Assistant Chief Engineer*; **Mohsin** *Project Engineer*; **Scott Berggren** *Chief Engineer*; **Jason Morin** *Project Engineer*

Gryphon Design Co.

GRYPHON DESIGN CO.

Brandon Griffin	**Antonio Araujo**	**Matthew McCormick**	**Chad Goodlow**	**Jason Gulledge**	**Matthew Niestroy**
Team Lead	*Research Lead*	*Design Lead*	*Production Lead*	*Quality/ Reliability Lead*	Analysis Lead

Airbus Intake Group

Allen , D., Mendez, A., Murillo, A., Tovar,M.
ME Senior Design

UNIVERSITY OF TEXAS ARLINGTON | COLLEGE OF ENGINEERING

Executive Summary

The Airbus Intake Group is working on designing a scoop attachment to improve incoming flow on a intake of a AS350B3 helicopter. A CFD analysis is being done on the intake to visualize the flow and find the proper flow characteristics.The goal is to design an attachment that will improve the pressure recovery of the intake to improve the engines power and efficiency.

Background

Obtaining better fuel economy, and increased safe operation of the AS350B3 lies in optimizing the flow at the compressor. The current AS350B3 static intake has a geometry with sharp edge causing a vortex. Using CFD tools, the team seeks to find an attachment best suited to increase pressure recovery.

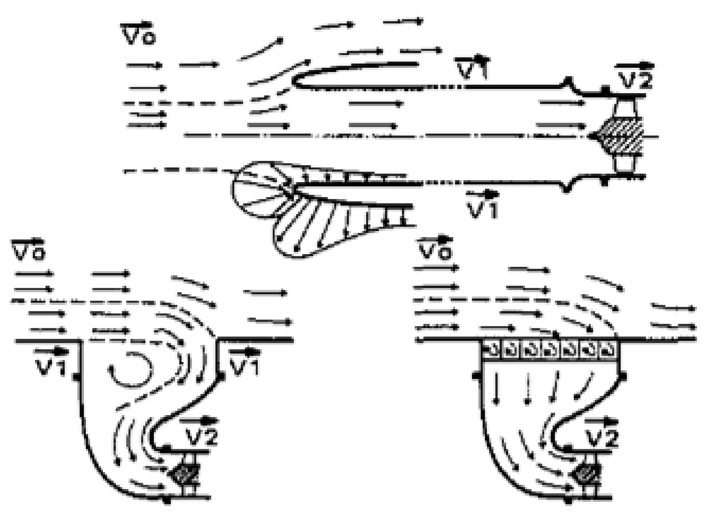

Figure 1. Static Intake (Bottom) vs Dynamic Intake (Top) [1]

Conceptual Design Phase

Design Specification

-Any attachment must have a distortion coefficient below 0.30, which is the engine acceptable range.

-Pressure Recovery needs to improve for all three conditions shown below in Table 1.

Table 1. Non-Attachment Intake Results

Flight Speed	Pressure Recovery	Distortion Coefficient
Hover	87%	0.26
60 Knots	55%	0.24
120 Knots	46%	0.39

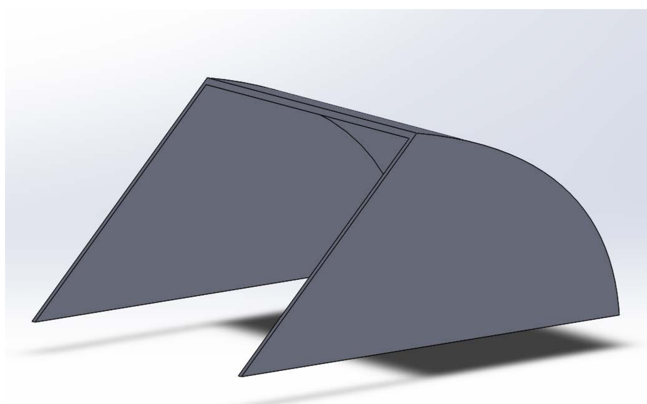

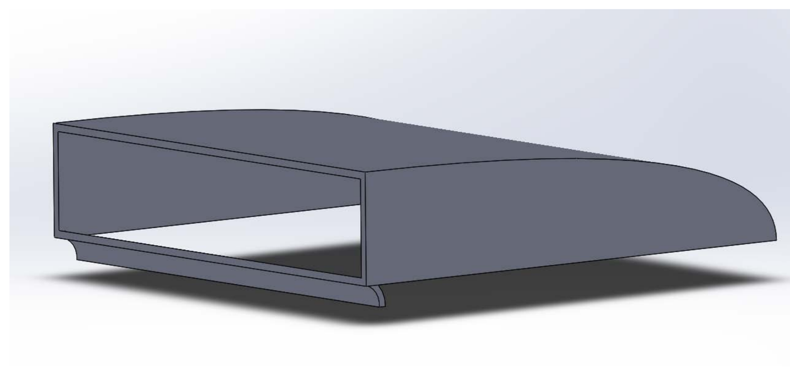

Detailed Design Phase

To obtain the desired results, the main concerns are pressure recovery and distortion at the inlet face of the compressor. To increase the pressure recovery a scoop that attaches to the top of the helicopter will be implemented. The scoop is designed to grab as much free-stream air for the turboshaft engine. The scoop will need guide vanes in order to manipulate the flow of the air to flow evenly into the compressor of the engine effectively minimizing the distortion coefficient.

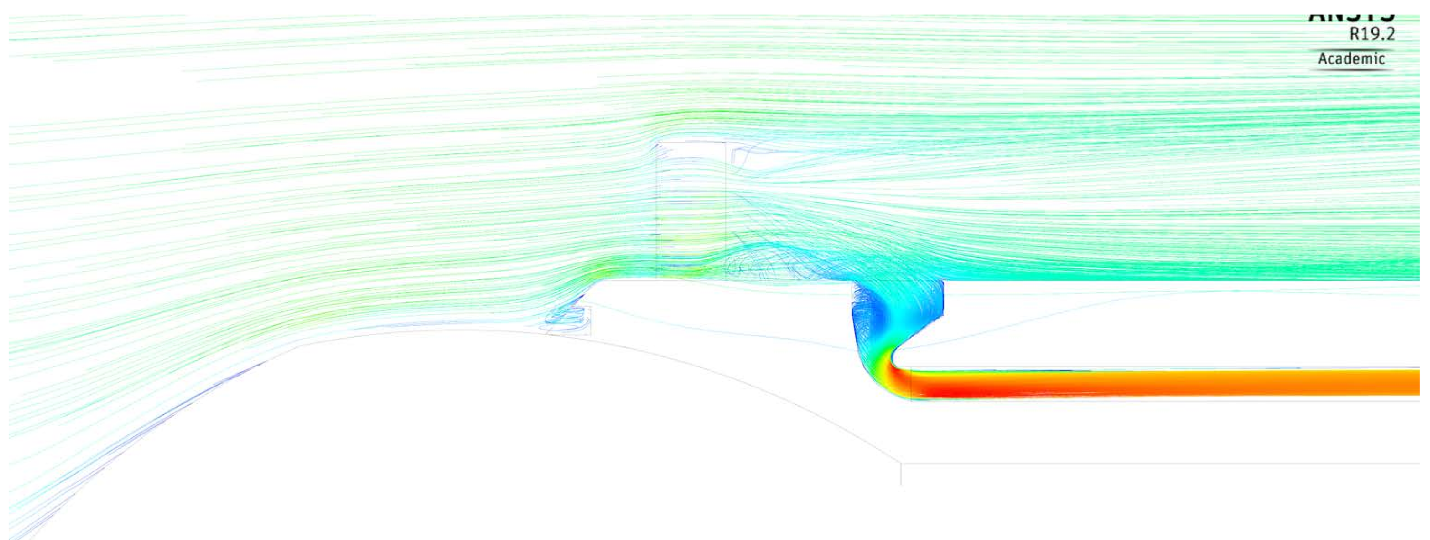

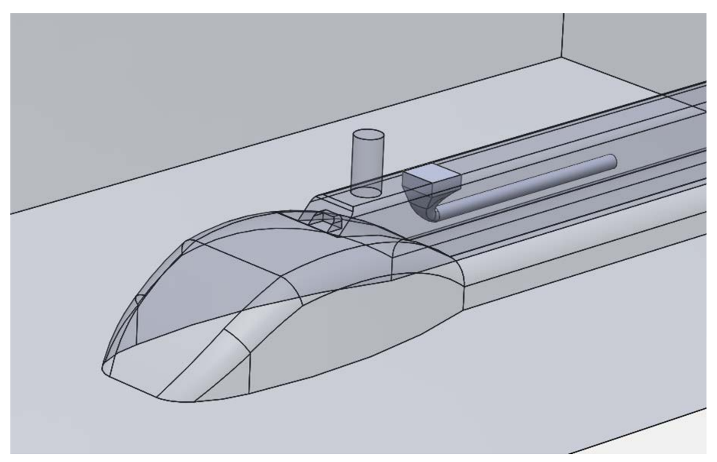

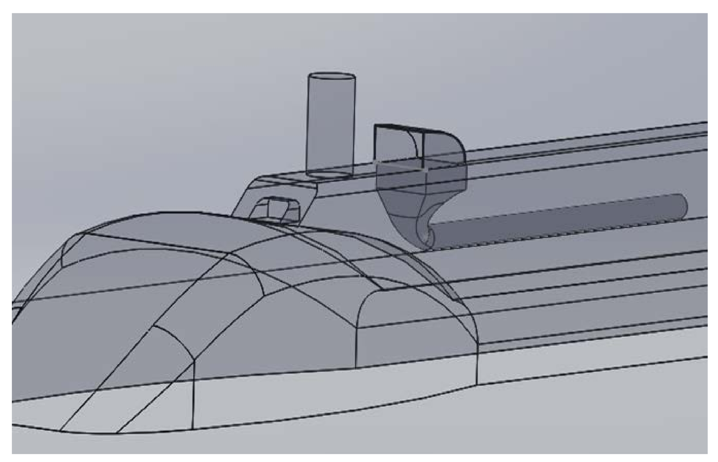

Prototype & Test

Using ANSYS FLUENT the team has begun to analyze ideas of scoops to improve the engines performance. The streamlines show that there is still vorticity where the air turns 90 degrees.

	Pressure Recovery	Distortion Coefficient
With Scoop	62%	.37
Without Scoop	46%	.39

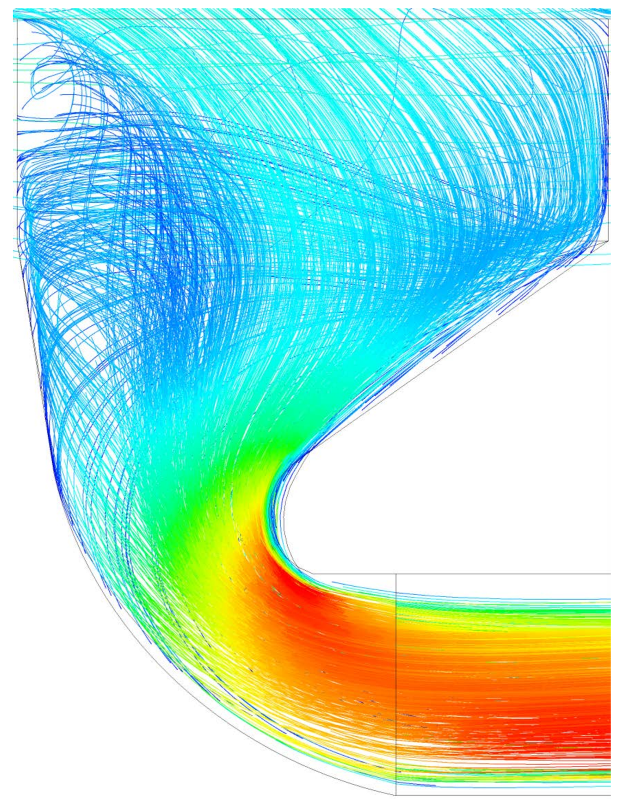

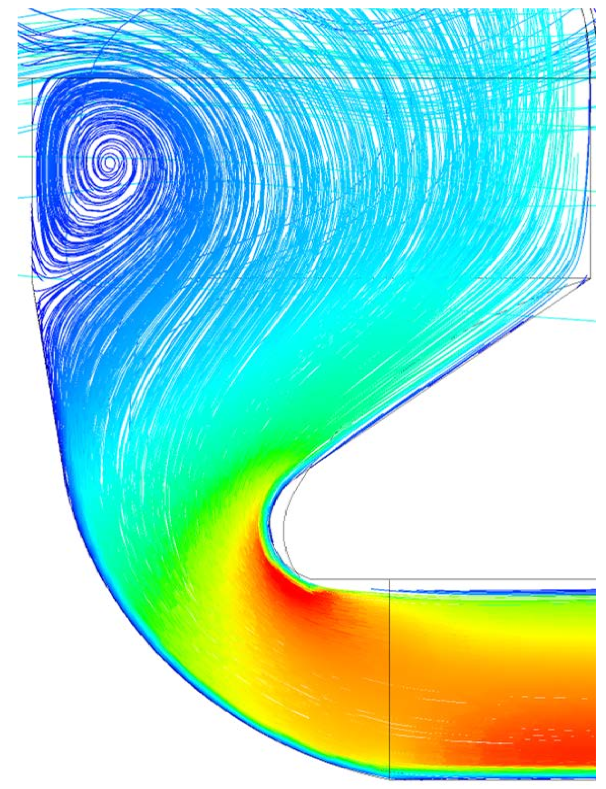

Conclusions

Improving pressure recovery will be the best way to obtain the highest power output. Minimizing distortion will cause the engine compressor to do less work which will not only increase the engine life, but help generate more power. The scoop design will improve both of the parameters and turn the static intake into a dynamic intake.

The Airbus Intake Group would like to gratefully acknowledge Dr.Robert Wood our faculty advisors. Likewise Mr.James Merkel and Mr.Denis Hamel of Airbus Helicopters for they're support.

References

1. Vuillet, A. Aerodynamic design of engine air intakes for improved performance. In Proceedings of the Sixth European Rotorcraft and Powered Lift Aircraft Forum, Bristol, UK, 16–19 September 1980.https://dspace-erf.nlr.nl/xmlui/bitstream/handle/20.500.11881/1834/ERF%201980-51.pdf?sequence=1
2. Roy,B., Pradeep, A.,Lecture 13 Turbomachinery Aerodynamics https://nptel.ac.in/courses/101101058/downloads/Lec-13ppts.pdf
3. Hazaveh, Hooman Amiri, and S.M Nima Shojaee. "Investigation of Total Pressure Distribution at Aerodynamic Interface Plane of an 'S-Shaped' Air Intake at Sideslip Condition." *International Journal of Natural and Engineering Sciences*, 1 June 2014, pp. 88–94

2019 UTA College of Engineering Innovation Day April 15, 2019

Real Time Clogging Indicator for an Inlet Barrier Filter System for an AS350-B3

Mata, E., Seay, D., Cervantes, E.
Mechanical Engineering Senior Design

EDETECH

AIRBUS HELICOPTERS

UNIVERSITY OF TEXAS ARLINGTON | COLLEGE OF ENGINEERING

Executive Summary

Helicopters operating near ground and in unprepared areas are susceptible to ingesting dust and particles, reducing turbine engine life. Inlet barrier filters effectively trap the unwanted elements but over time become increasingly clogged, increase pressure losses and reduce engine power available.

In order to maximize filter life and operate at maximum performance available, a real-time cockpit clogging indicator is required. Clogging is calculated from the following independent parameters: pressure loss across the medium, airspeed, outside air temperature, pressure altitude, and engine gas generator speed.

The clogging indicator created provides a scale representing the filter state ranges as percentage of the predetermined critical pressure drop The clogging status uses a model for the mass flow as well as a pressure model for different flight regimes – all based on available test data provided, an experimental data that was tested for.

Background

Currently, there is no real time indicator for the AS350 B3 helicopter (Figure 1). There is only a maintenance light that activates when a critical pressure differential is experienced by the sensor in the IBF system.

Being able to have a real time clogging indicator can give pilots a way to verify aircraft performance as well as give a competitive market advantage for manufacturers

A pressure differential increase correlates to a clogged filter. The different parameters that were found to have a role in the can be seen in Figure 2.

Figure 1. AS350 B3/H125 Helicopter and IBF System

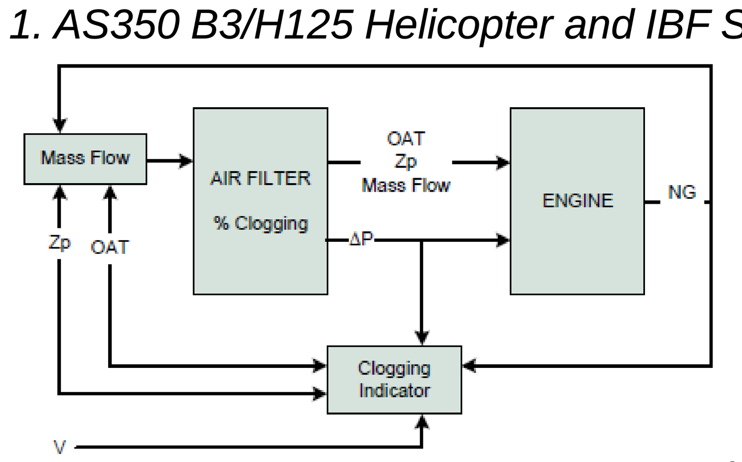

Figure 2. Contributing Parameters Clogging indicator

Conceptual Design Phase

The data that was provided contained a pressure differential readings during different flight phases. The first phase was to the design required the creation of an accurate pressure model that will emulate as closely as possible the pressure differential sensor readings that the data. In order to do this, a mass flow model was necessary.

It was determined that the pressure differential model needed to be a function of the parameters that the test flight data provided.

Once the pressure model was completed, it was assumed to be good enough to use as a contributor to the next step – creating a clogging model. This clogging model was then to be used for the clogging indicator.

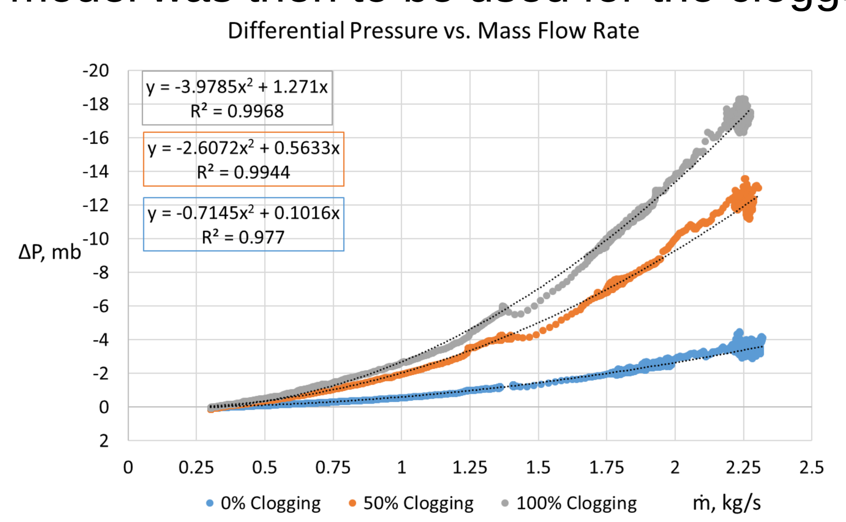

Figure 3. Test Flight Data for Starting Flight

Where, $\dot{m} = 0.0264N_{red} + 0.302$

With, $N_{red} = 0.017N_G^{1.87}\theta^{-1.53}\delta^{1.24}$

And where, $\Delta P_{Model} = k_2\dot{m}^2 + k_1\dot{m}$

With, $k_1, k_2 = f(clogging)$

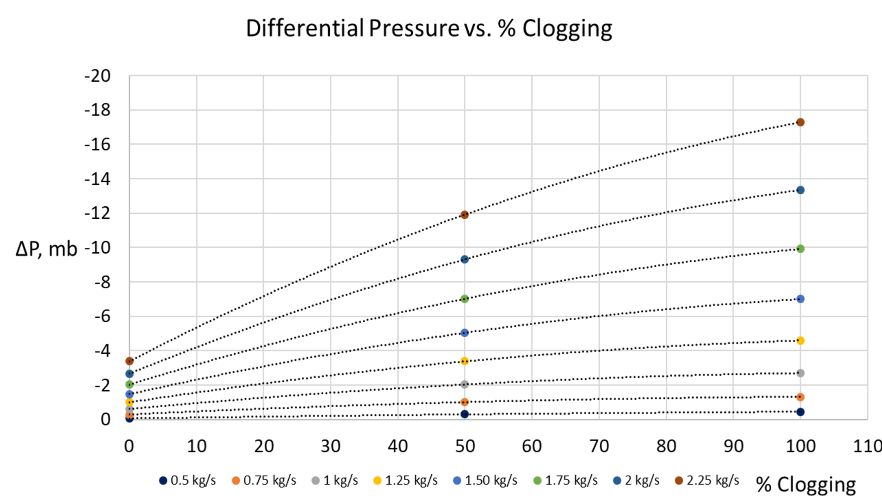

Figure 4. 1st Iteration of Clogging Indicator

- For an isolate and calculated mass flow rate, the pressure sensor can be used to find the clogging percentage.

Detailed Design Phase

It was determined that when programming the clogging indicator, logic structures would be complex and complicated if the first approach was taken. Thus the problem was broken down further to simplify.

The pressure differential reading was a combination of two sensors. The contributing factor were found. This yielded the following results.

Starting,

$$\Delta P_{Model} = \Delta P_{IBF} = P_{S,Inside} - P_{S,Outside}$$

Considering Filter Clogging contribution

$$\Delta P_{IBF(Inside)} = (k_1 * \dot{m}^{k_2})(1 + x_1 * Clogging^{x_2})$$

Furthermore,

$$\Delta P_{IBF(Outside)} = f(CAS) + f(Zp)$$

Combining,

$$\Delta P_{Model} = \Delta P_{IBF}$$

$$= (k_1 * \dot{m}^{k_2})(1 + x_1 * Clogging^{x_2}) + f(CAS) + f(Zp)$$

Ultimately,

$$Clogging = \left[\frac{\Delta P_{IBF} - f(CAS) - f(Zp)}{x_1(k_1 * \dot{m}^{k_2})} - \frac{1}{x_1}\right]^{1/x_2}$$

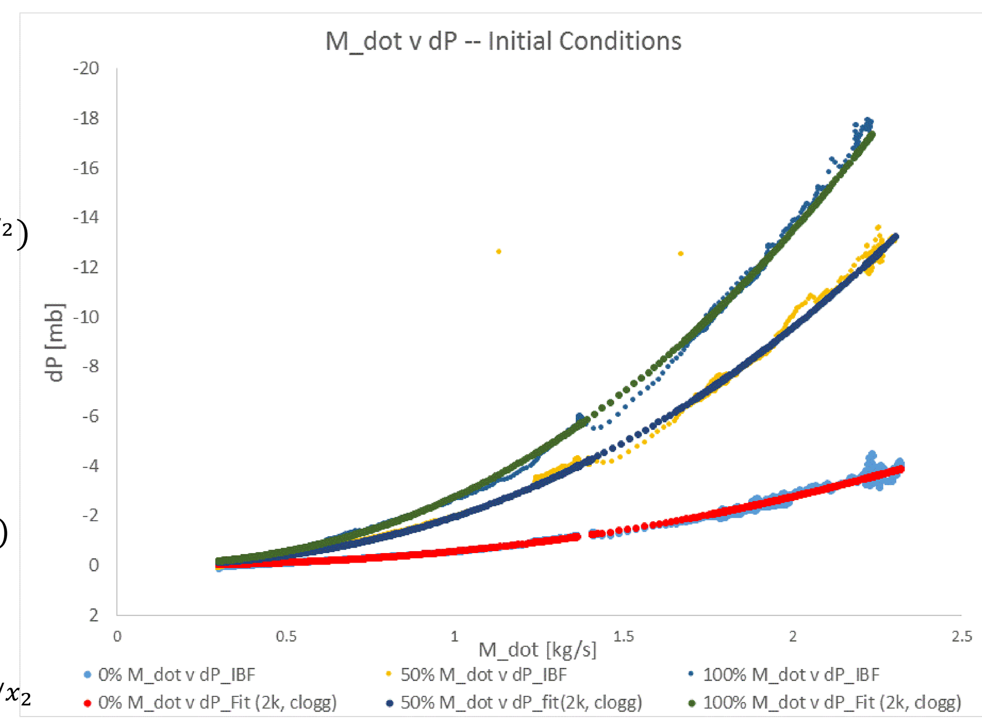

Figure 5. Clogging equation compared to Test Data for Mass Flow contribution

This process was done using Excel's Equation solver features. The outside sensor contributing parameter are known but there has yet to be a convergence on the ideal values that will be used in the equation.

Prototype & Test

Our team needed a computing system capable of rapidly solving an extensive amount data using of very specific equations. Thus, the team utilized Excel and MATLAB to derive and program the clogging indicator and the corresponding equation. There is still improvement that is needed. It is possible that the final prototype will have a complex logic and conditionally driven code Therefore, flexibility is important.

The team implemented this current clogging equation into MATLAB to prepare a prototype of the indicator before integrating it onto hardware. With the endless visual capabilities of MATLAB, we were able to display our indicator in real-time using test flight data. Furthermore, the process of using and Arduino Uno R3 and a Elegoo Uno R3 display have been explored.

Figure 7. Arudino Uno R3 and Elegoo Uno R3 Hardware

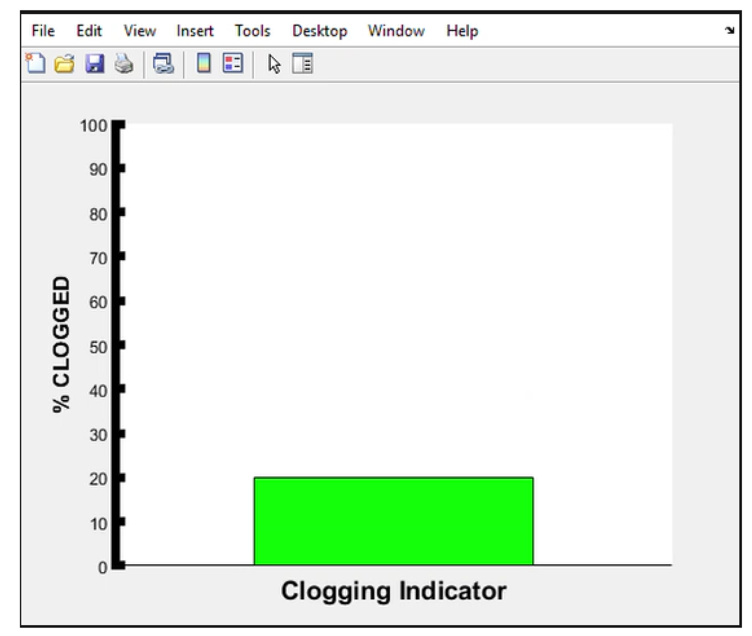

Figure 8. MATLAB Clogging Indicator

Conclusions

The current clogging indicator is able to model the clogging of an inlet barrier filter for flight regimes in which mass flow rate and clogging contributions are the main contributors to the pressure IBF pressure differential sensor – more specifically during engine start, liftoff, idle to flight, and hover flight regimes.

Furthermore, development of the pressure model are necessary in order to then improve the clogging equation. The function of the outside differential sensor contributing parameters need to be converged on. The use of the hardware has been started and partially accomplished, however it is yet to be accurately competed.

This current status of the project and prototype is currently a partial fulfillment of the specifications set by the sponsor. In the near future, it is expected to converge on the most accurate pressure model and clogging indicator.

References

[1] Donaldson Filtration Solutions, "Instructions for Continued Airworthiness - Inlet Barrier Filter system for the Eurocopter France AS350B Series Helicopters," Donaldson Filtration Solutions, 2014.
[2] D. Hullender, R. Woods and Y.-W. Huang, "Dingle Phase Compressible Steady Flow in Pipes," Journal of Fluids Engineering, 2010.
[3] J. Merkel and D. Hamel, "Clogging Indicator System for and AS350 in Collaboration win UT Arlington Mechanical Senior Design -- Technical Note Revision II," Airbus, 2018.
[4] J. Merkel and D. Hamel, "Clogging Indicator System for and AS350 in Collaboration win UT Arlington Mechanical Senior Design -- Technical Note," Airbus, 2018.
[5] Otto Freund, "Air Speed Indicator Calibration Measurement Position Error Correction - PEC," in European Telemetry and Test Conference, 2014.
[6] B. Bekesi, "Attitude Instrument Flying in Helicopters," Repulestudomanyi Kozlemenyek, 2010.
[7] N. Bojdo and A. Filippone, "Operational Performance of Inlet Barrier Filters for Rotorcraft," The Aeronautical Jurnal, vol. 116, no. 1182, pp. 847-869, 2012.
[8] V. Hwa, "Test and Evaluation of an Inlet Barrier Filter to increase Engine Time-on-Wing for the Bell Boeing V-22 Offspray Tiltrotor - Thesis," The University of Texas at Arlington, Arlington, 2015.
[9] N. Bojdo and A. Filippone, "Effect of Desert Particulate Composition on Helicopter Engine Degradation Rate," The University of Manchester.

Integrated In-Wheel Powertrain Design

Herring J., Lamotte-Dawaghreh J., Pechal L., Pugliese T., Smith M., Tolar G.
ME Senior Design

Executive Summary

NextGen Drive is a team of senior Mechanical Engineering students working with Dr. Yawen Wang in the Mechanical Engineering Department at The University of Texas at Arlington to research and develop the design of an integrated in-wheel electric motor powertrain solution for an electric vehicle that offers increased energy efficiency, delivers superior vehicle performance, and improved safety over traditional automobiles.

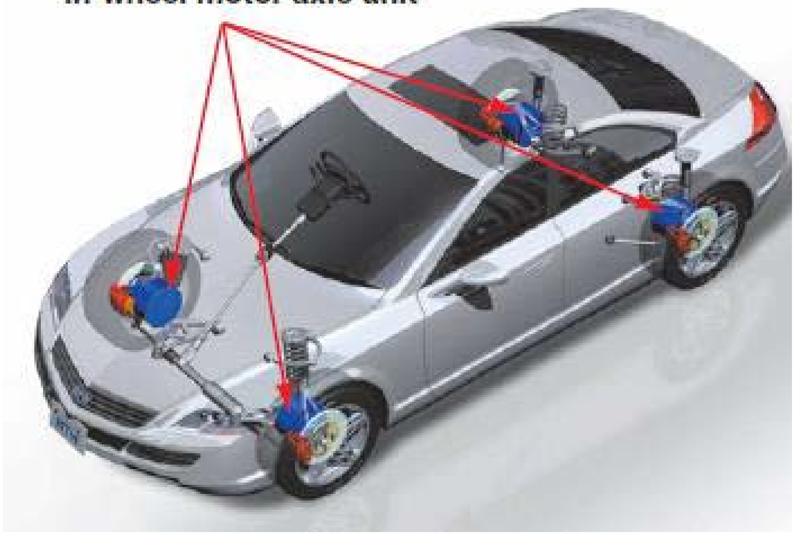

Figure 1. In-Wheel Drive

Background

Emission standards continue to be tightened due to concerns over improving environmental stewardship. Over half the carbon monoxide, and nearly 25% of the hydrocarbons released into the air in 2013 were attributed to transportation [1].

The primary benefit of In-Wheel Drive is that each wheel is independently supplied necessary torque. This is termed "torque vectoring". Torque vectoring achieves the same that a differential does to retain vehicle stability, but instead of using gears that will generate heat to do this, electronic controllers would be used to vary the torque being supplied to each wheel.

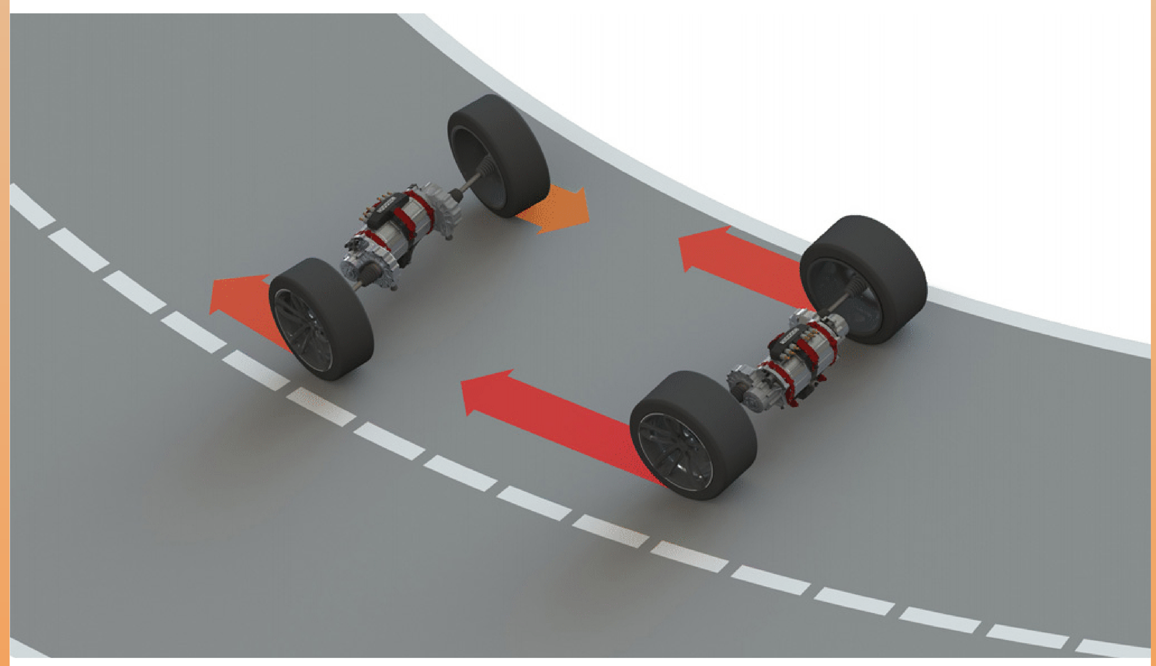

Figure 2. Torque Vectoring [2]

Conceptual Design Phase

NextGen Drive has developed a preliminary conceptual design of the mechanical components of an electric drive system that fits inside the wheel of a regular vehicle.

Table 1. Design Performance Requirements

Constant Velocity	Accelerating
100 mph, 0° grade	4 m/s^2 at 5 mph
85 mph, 5° grade	3 m/s^2 at 30 mph
60 mph, 8° grade	1.75 m/s^2 at 50 mph
30 mph, 18.4° grade	1 m/s^2 at 60 mph

The design process began with developing a house of quality to define clear customer requirements and derive the corresponding engineering characteristics our system requires in order to best meet our client's needs. The next step was to define system performance requirements. This large engineering task required a substantial amount of research regarding current electric vehicle standard performance and analysis.

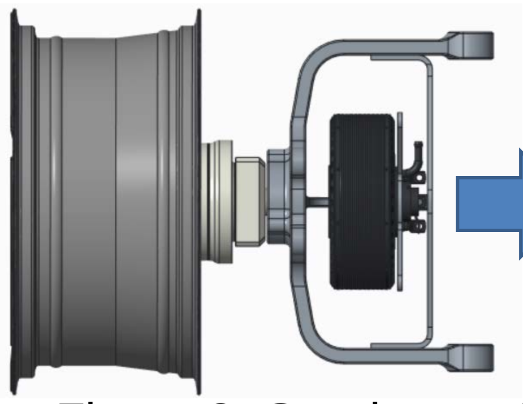

Figure 3. Gearbox

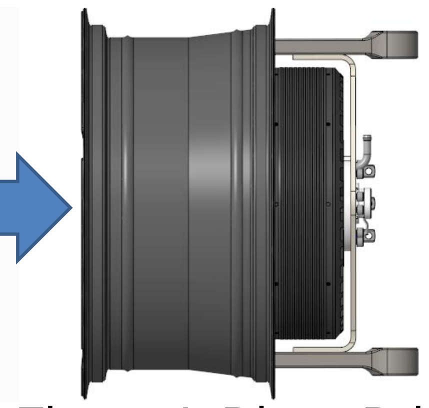

Figure 4. Direct Drive

Fig. 5. Hub Assy.

Fig. 6. Torque Shaft

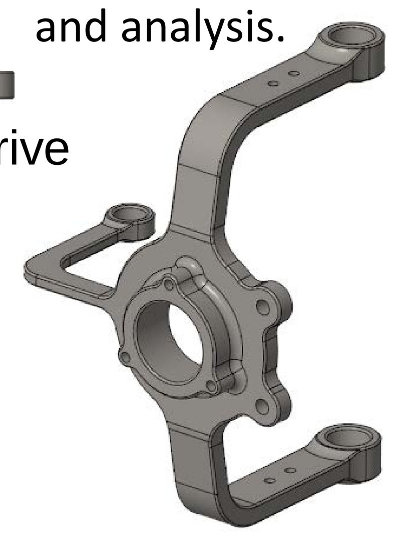

Fig. 6. Knuckle

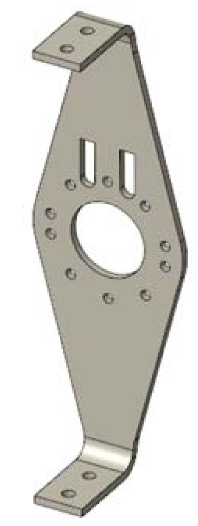

Fig. 7. Motor Mount

Detailed Design Phase

Building upon the preliminary conceptual design, our team is developing a steering knuckle that allows the elbows to pivot independently of the rest of the in-wheel assembly, moving the steering axis directly in-line with the wheel, vastly improving handling performance of the vehicle.

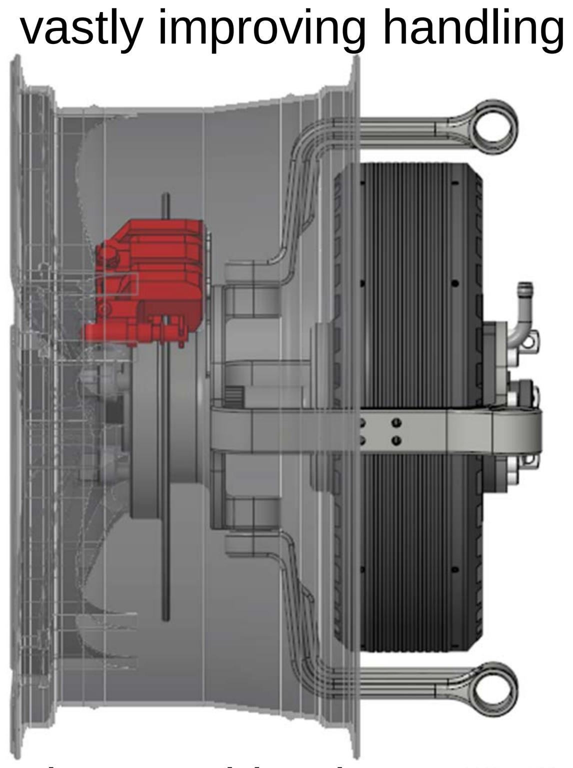

Fig. 12. Side View

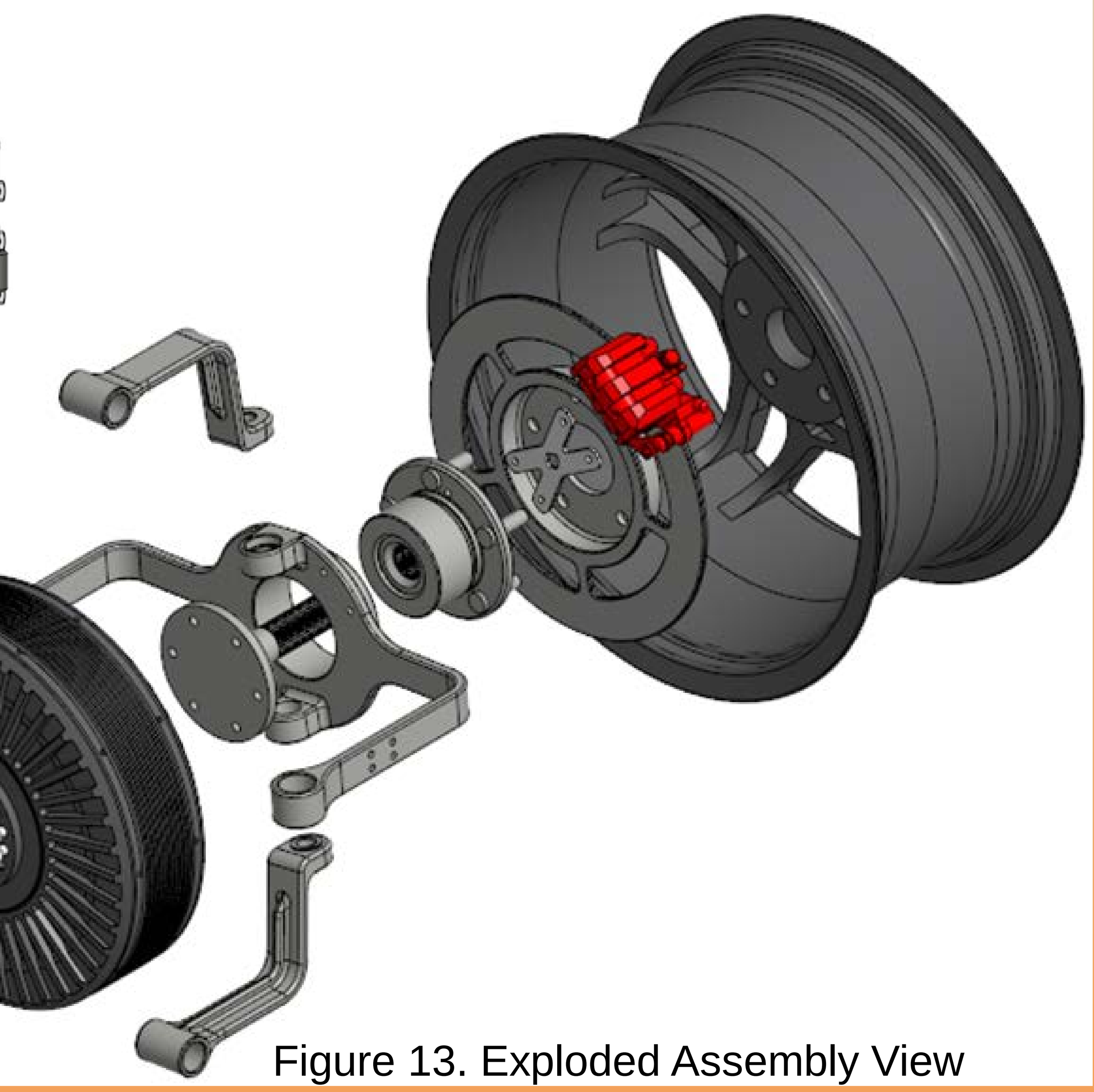

Figure 13. Exploded Assembly View

Analysis and Prototype

ANSYS structural analysis was conducted to verify that designed structural components could withstand the experienced loading to an industry standard factor of safety. Once the design was substantiated with analysis results, a geometrically representative prototype was 3D printed on a Prusa i3 3D printer.

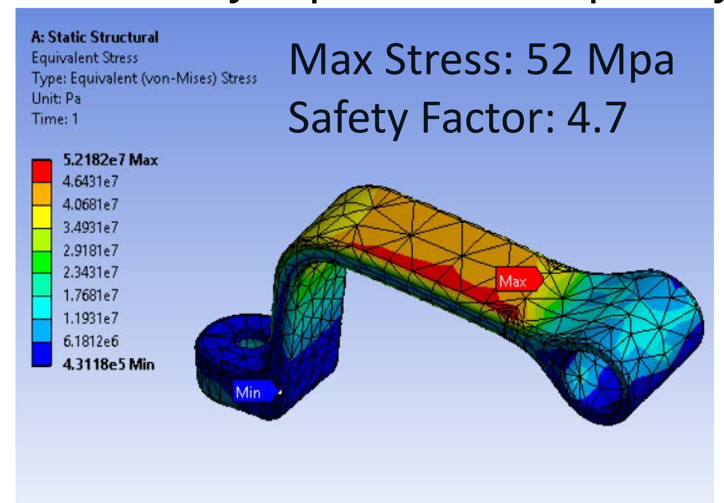

Figure 8. Upper Elbow

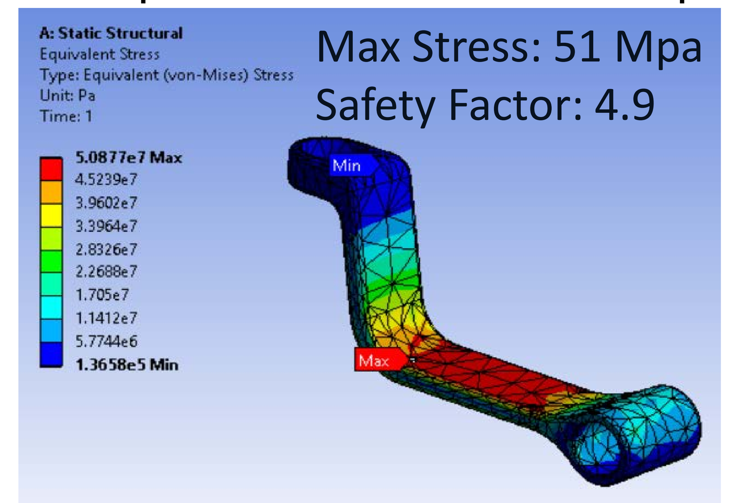

Figure 9. Lower Elbow

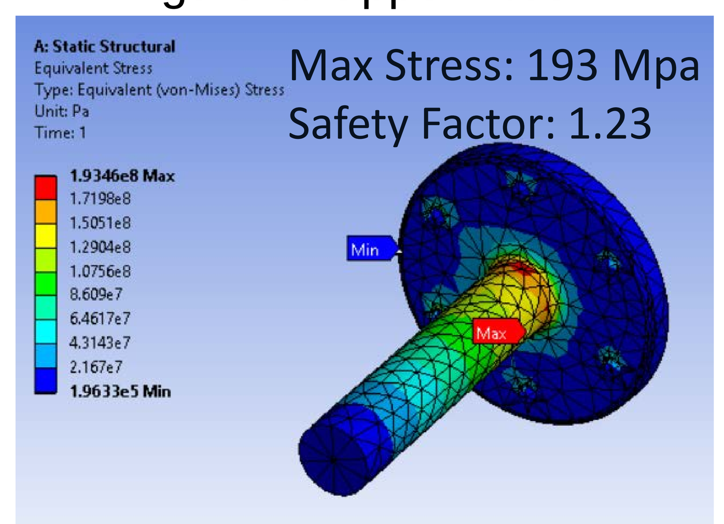

Figure 10. Torque Shaft

Figure 11. Prusa i3 mk3 [3]

Conclusions

Altogether, our in-wheel motor design exceeded our client's goals in terms of electric drivetrain performance. The design will allow for the vehicle to not only outperform typical electric car, but also outperform most commuter cars in the market. Our design process was one of iteration in terms of everything from motor selection down to the structural design needed to provide the maintainability the vehicle's dynamics. Moving forward, we will be completing the fatigue analysis as well as completing a quarter-car analysis, after which we will complete the engineering drawings and obtain a finalized CAD product. The NextGen Drive team would like to give the upmost thanks to our faculty advisor Dr. Yawen Wang and Dr. Woods for giving us support during the design process.

Dr. Yawen Wang
Faculty Advisor

References

[1] UCS, "Vehicles, Air Pollution, and Human Health" https://www.ucsusa.org/clean-vehicles

[2] "TecnicaMania: Come Funziona Il Torque Vectoring." *Toute L'actu, Essais Et Vidéos De Supercars-Supercar Team*, www.supercarteam.com/tecnicamania-come-funziona-il-torque-vectoring/.

[3] "Prusa i3 mk3 3D Printer", https://www.prusa3d.com/original-prusa-i3-mk3/

2019 UTA College of Engineering Innovation Day **April 15, 2019**

Electric Scooter

Garcia, Alex ● Malke, Travis ● Navarette, Nick ● Rush, Cooper ● Smith, Alexander

Smith, Jeremy ● Woods, Matt

ME Senior Design

UNIVERSITY OF TEXAS ARLINGTON | COLLEGE OF ENGINEERING

Executive Summary

This engineering design project is undertaken by 6 Mechanical and 1 Electrical Engineering undergraduate students at The University of Texas at Arlington. The goal of the project is to design and manufacture a fat-tire electric trike (FTET).

To facilitate an effective and successful engineering design, a comprehensive list of customer requirements were transformed into the following specifications.

- Accommodate the 95% male and 5% female.
- Provide a 30-mile range when operated at full power for an hour
- A long lasting and reliable battery with quick recharge time and chemistry of $LiFePO_4$
- Independent rear suspension to handle like a motorcycle
- Constructed of 4130 Chromoly Steel
- Utilize commercial off the shelf products to minimize cost and time

Background

A survey by statista.com reveals a boom in the plug-in electric vehicle sales in the United States between 2017 and 2018 [1]. An online article by marketwatch.com states, "The electric scooter market is anticipated to reach over USD 51,324 million by 2026" [2]. Statistics show that as electric vehicle technology becomes more efficient and cost-effective demand for electric vehicles is going up.

Our client wants to be part of this increasing market trend. Our in-depth market analysis of electric scooters revealed two main categories, the standing collapsible and seated rigid frame. Rather than focus on the main stream our client wanted to focus on a niche market. Our design is aimed for two specific groups, industrial warehouses and golf cart communities.

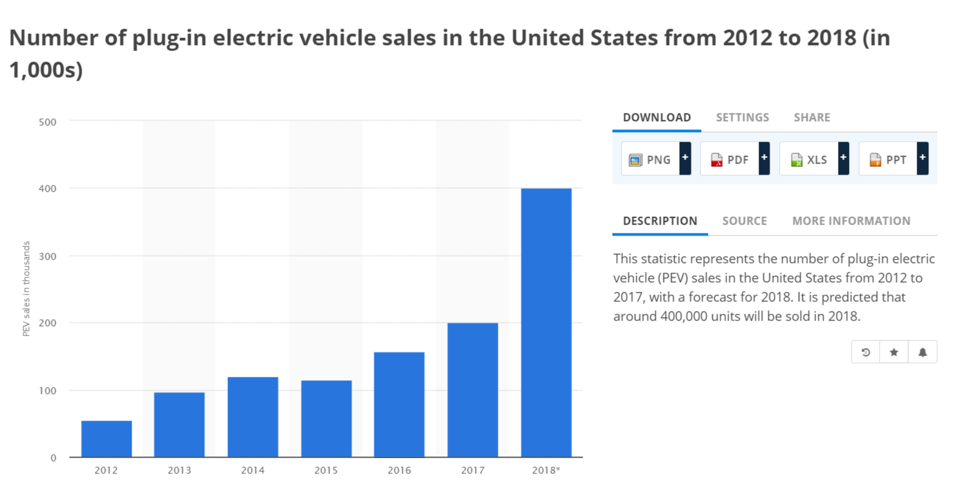

Figure 1. PVEV Sales 2012-2018

Conceptual Design Phase

Cage Consulting provided our client with an in-depth overview of the electric scooter market. This helped the team to attain a better understanding of what the client wanted. Our client, Dr. Robert Woods the founder of UTA Racing Formula SAE, desired something other than the traditional small two-wheel scooter the market was currently offering. Our team proposed a design inspired by the German engineered Scrooser™ , differing in that it has two rear wheels with independent rear suspension to handle like a motorcycle.

Figure 2. Inspirational Design Scrooser™

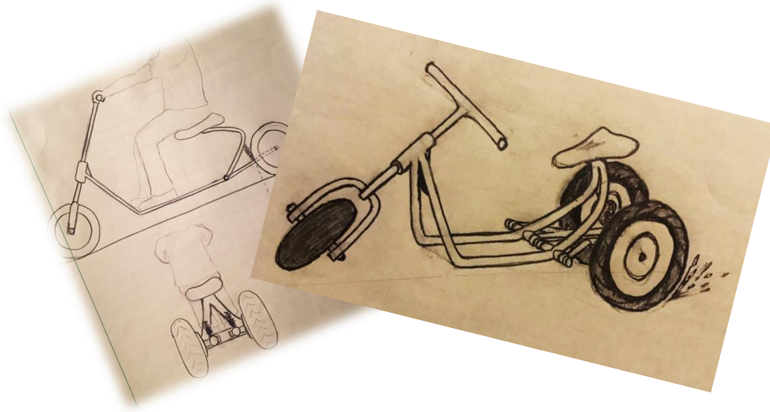

Figure 3. Conceptual Designs

Figure 4. Phase I Design

Detailed Design Phase

Our chassis design utilizes 1½ inch 4130 Chromoly Steel tubes with 0.049-inch wall thickness except for the front stem being a 2-inch diameter. The rear swingarms are designed with a 0.095 wall thickness to provide a higher safety factor. The rear swing arms are one of the distinguishing factors in our design. The swingarm design provides independent rear suspension that allow the rider to lean in to a turn as if operating a two wheeled motorcycle.

With large tube diameters and three large 165/55 12-inch tires our design is meant to display power, strength, and durability. To achieve this our design utilizes a 48V battery, two Kelley controllers and two 12-inch 2000W hub motors.

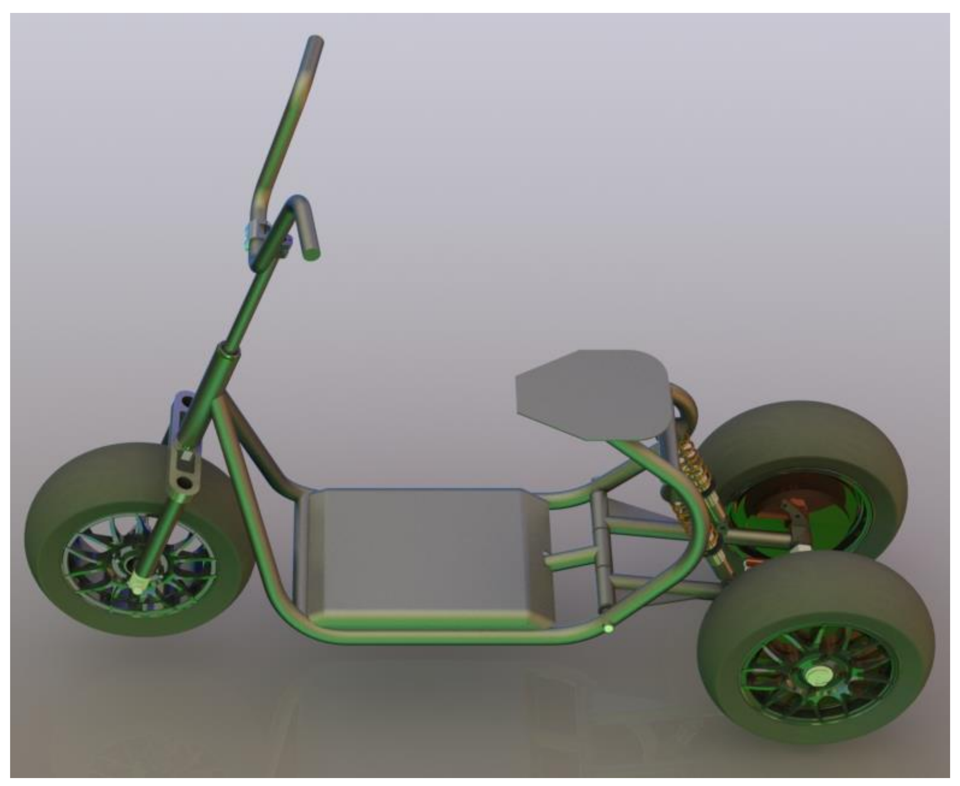

Figure 5. Current Solid Model Rendering

Figure 6. Independent Suspension

Prototype & Test

Prior to prototype fabrication, solid models of the chassis and rear swing arms were put through numerous tests using ANSYS software. ANSYS claims that their "With ANSYS' Multiphysics solutions, products can be virtually tested under real-world operating conditions that typically involve simultaneous, multiple physical loads" [3]. Dr. Kent Lawrence, the Universities foremost authority in computer aided engineering and FEA, was consulted during this process to ensure testing was done correctly. Test results confirmed that none of the components of the scooter yield under max loading conditions. Material Test Reports from our chassis and swing arm vendor show the tubing selected to have higher yield strength than anticipated from our stress analysis tests in ANSYS.

Currently, the project is in the prototype assembly phase. All major components of the scooter both COTS and fabricated are being assembled and welded. The prototype is on schedule for final delivery of 4/30/2019.

Figure 7. Chassis & Swingarm

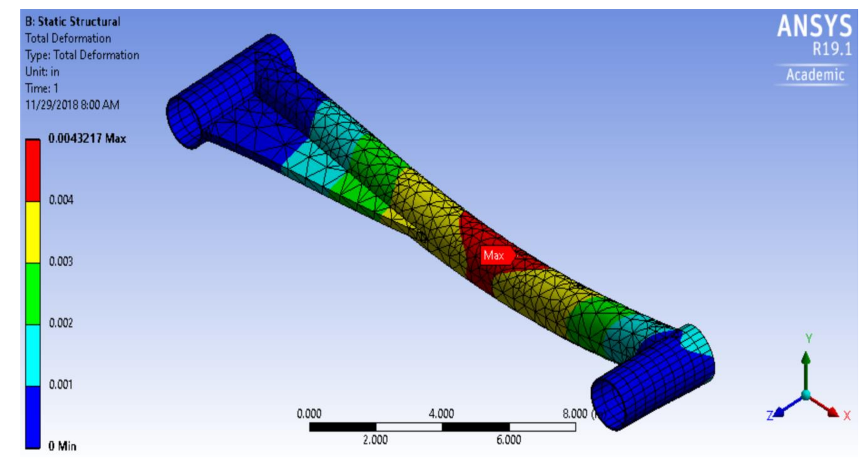

Figure 8. Swingarm Stress Test

Conclusions

In conclusion, we have met and exceeded the initial scope of this project and are on schedule to meet all the client's requirements. We would like to thank our client and advisor Dr. Robert Woods. He has advised our team with guidance and wisdom. He challenged us in his role as a client and boss and he tested us as future engineers requiring that we give more and rise above the rest. He encouraged us to make many of the choices that led to our final design and with our choices came accountability. Within the accountability lie logic, math, science, physics, and engineering principles that have made this an undeniably unique senior design project. We feel that this project greatly reflects the wide range of engineering courses taken in our undergraduate careers. It has required principles learned in engineering design, statics, dynamics, solid mechanics, properties of materials, thermodynamics, circuit analysis, mechanical design, fluid mechanics, CAE, dynamic systems and modeling, and intro to manufacturing.

References

[1] "U.S. - PEV Sales 2018 | Statistic." *Statista*, www.statista.com/statistics/801263/us-plug-in-electric-vehicle-sales/.

[2] By. "Electric Scooter Market Global Potential Growth,Share,Demand and Analysis Of Key Players Forecasts to 2026." *MarketWatch*, 6 Feb. 2019, www.marketwatch.com/press/release/electric-scooter-market-global-potential-growthsharedemand-and-analysis-of-key /players-forecasts-to-2026-2019-02-06.

[3] "Vehicle Simulation for Quality Assurance & Safety." *ANSYS*, www.ansys.com/solutions/solutions-by-industry/automotive/quality-and-reliability.

2019 UTA College of Engineering Innovation Day **April 15, 2019**

3D Printed Aircraft (Wing)

Joshlin, T., Agolua, B., Iyer, K., Abusalah, S., Ahmed, Z., Montoro, M., Diya, N.

MAE Senior Design

UNIVERSITY OF TEXAS ARLINGTON | COLLEGE OF ENGINEERING

Introduction

Forward Air was hired by Stratasys to conduct research and development regarding Additive Manufacturing through the design of a 3D printed aircraft. Using Additive Manufacturing, many of the standard processes associated in designing and producing an effective model are eliminated to achieve cost effectiveness and time reduction. Additionally, Additive Manufacturing can allow for the implementation of complex geometric shapes due to its unique fabrication processes. Techniques such as sizing and topology optimization were performed to ensure the structural stability and lightweight design of the model before implementing it in 3D modeling. This project is separated into divisions which are the aircraft wing and the fuselage.

Background

This Project is intended to demonstrate the viability of fused deposition modeling as a prototyping method of thin walled structures. This is a legacy project which has been handed down from previous design teams and this project is a continuation of the design. FDM is a major promising manufacturing technique which enables the creation of lighter, stronger parts through the fusing of support and building material. This project is intended to show its viability and that a thin walled structure can be prototyped with zero to minimal post processing.

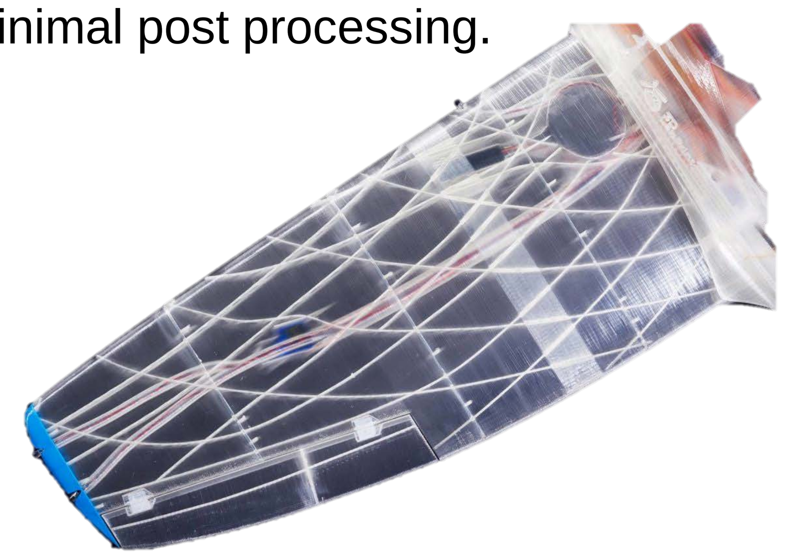

Figure 1: 3D Printed Wing example

Conceptual Design Phase

The DG-1 aircraft was chosen for design and analysis due to its relatively high aspect ratio wing. The model was imported into a cad modeler from OpenVSP. In the conceptual design phase, the team mainly utilized the loading conditions derived from other teams. The force and the bending moment derived from the discretization were applied to the quarter chord of each bay. The team also performed extensive research on the software used in this project namely, Altair Hyperworks for optimization and analysis, SolidWorks for CAD modeling, and INSIGHT for printing and slicing.

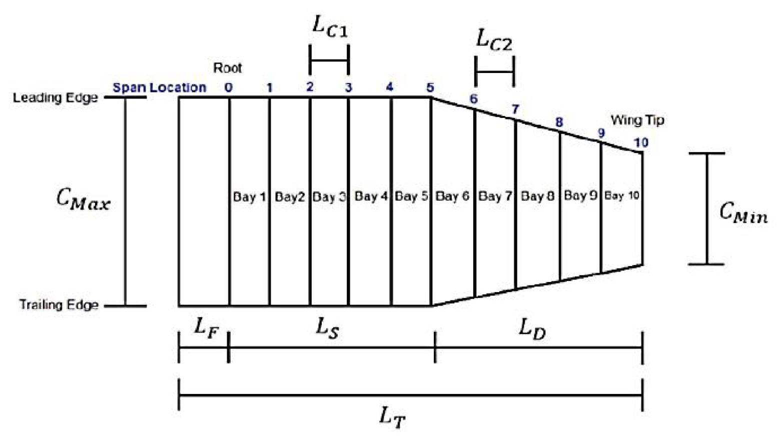

Figure 2: Division of the wing into bays

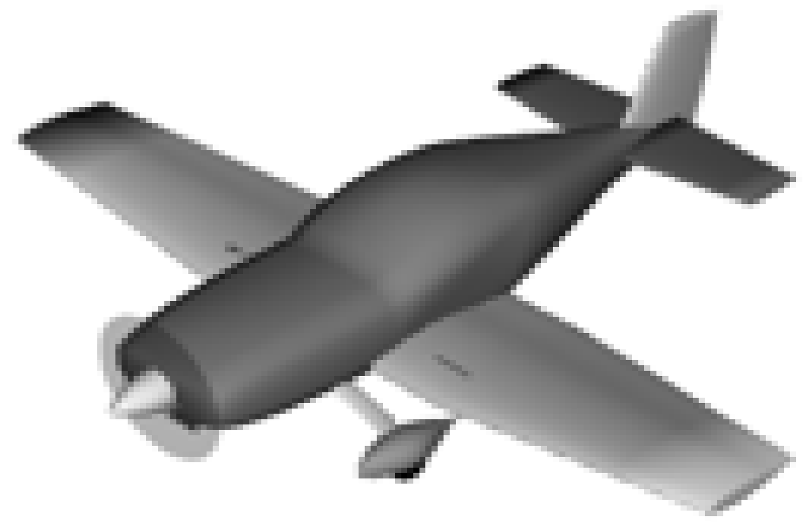

Figure 3: DG-1 Aircraft

Detailed Design Phase

The team performed sizing and topology optimization in Altair Optistruct to design the ideal pattern of the stiffeners for the given loading conditions. The objective of the topology optimization was to minimize the weighted compliance of the wing while constraining the final volume fraction to a specified value. Since no one iteration produced the intended results, the final stiffener pattern was obtained by interpolating the results from several iterations. Sizing optimization was done to determine the thicknesses of the skin and the stiffeners. To aid the proper connection of the wing and the fuselage, carry-through joints were designed. The 45 degree supports were added to account for drooping. The empennage is the horizontal and vertical stabilizers and it provides longitudinal stability. A male joint is present to overcome the limitations of the test bed. Stiffeners were added in the empennage by collaborating with the 3D printed Fuselage team.

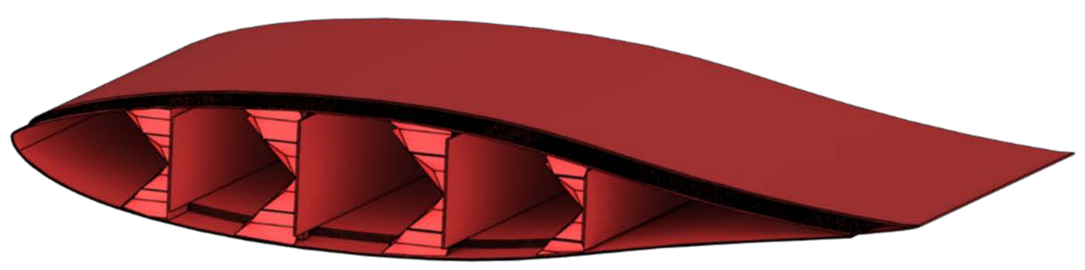

Figure 4: Carry-through joint

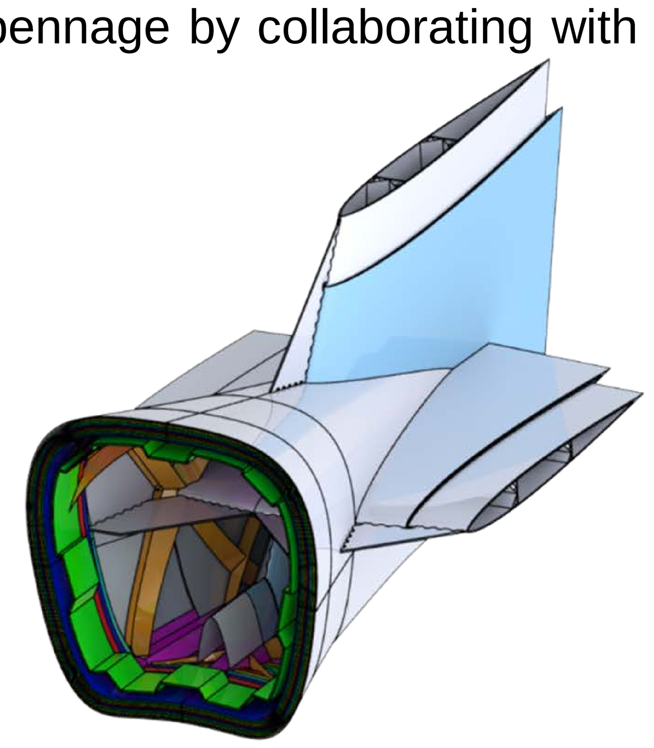

Figure 5: Empennage

Prototype

The topology and the sizing optimizations were conducted in Altair Optistruct. The internal stiffeners were modeled after interpolating the results from various topology optimization results. The largest displacement was found to be 0.04076 inches at the wing tip and the highest Von Mises stress was found to be about 140 psi at the root.

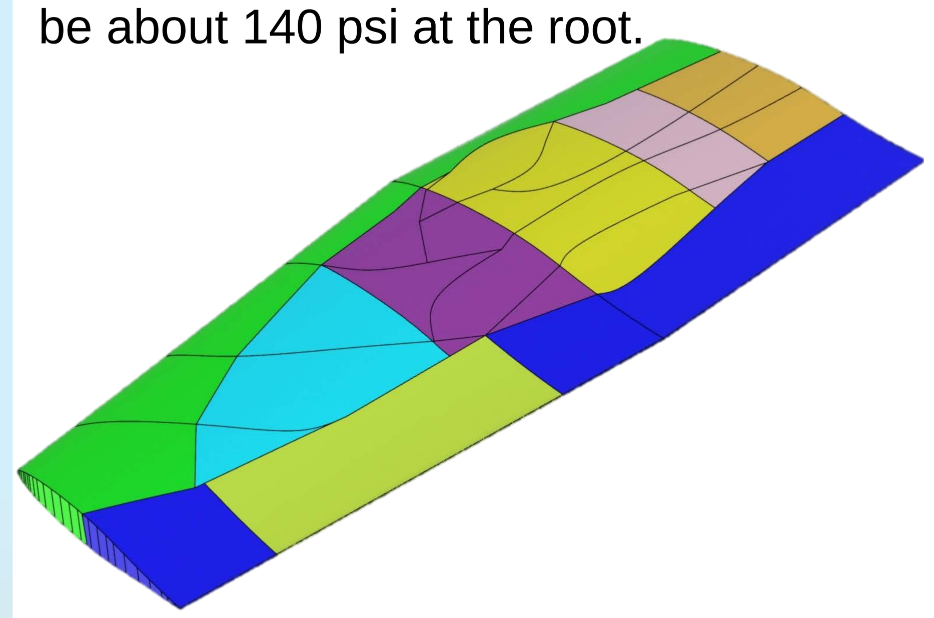

Figure 6: Sectioned wing

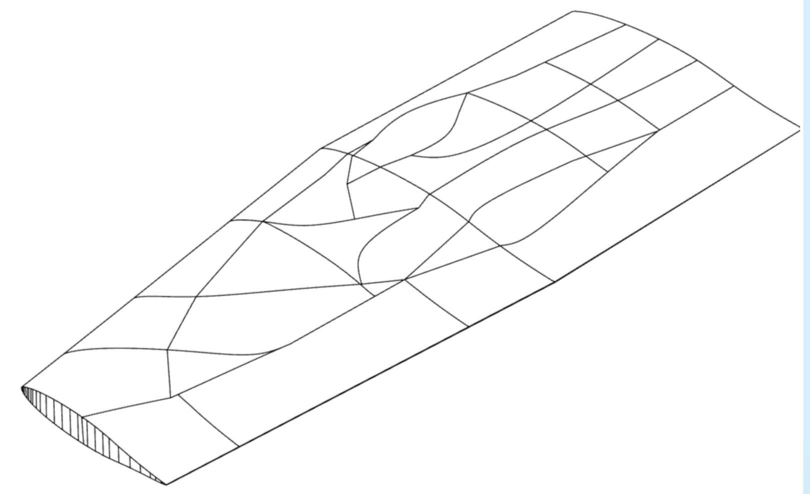

Figure 7: Internal stiffener

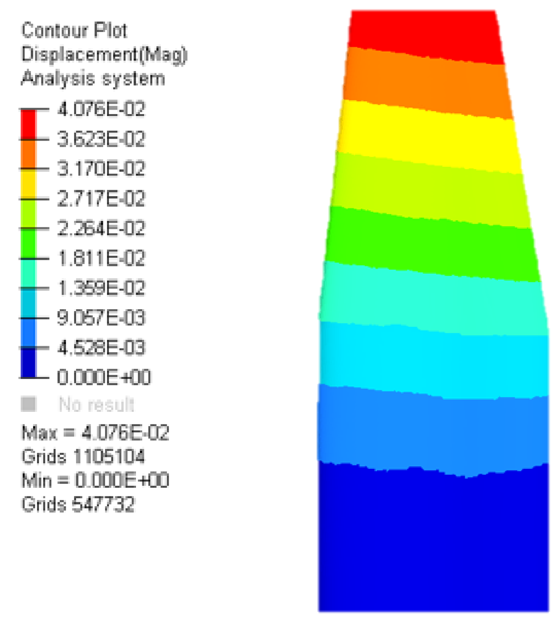

Figure 8: Displacement contours- Aileron deflection down-0.0476 in max

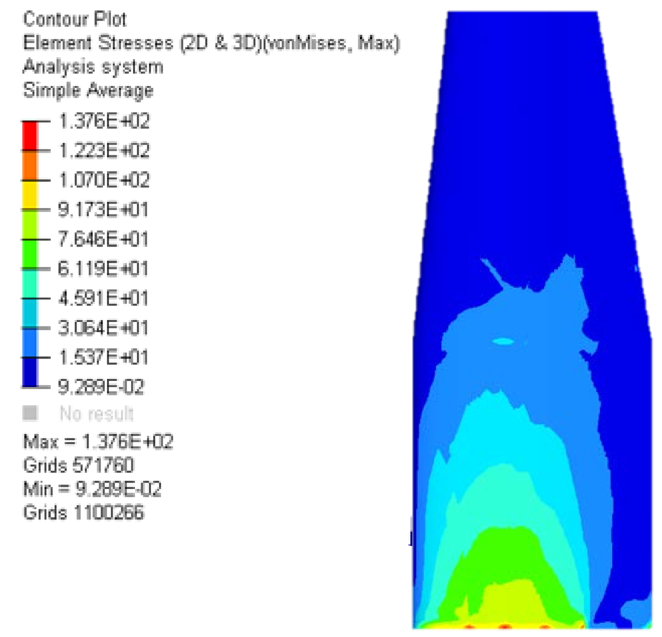

Figure 9: Stress contours- Aileron deflection up- ~140 psi max

The stress and the sizing results will be used to decide the thicknesses of the wing skin and the stiffeners across each section. These thicknesses will be modeled as additional layers and the wing will be modeled for printing.

Conclusions

With the help of our client and the assistance and guidance of Dr. Taylor, this team has succeeded in completing a design of a aircraft wing optimized for improved printability. However, issues such as overlapping surfaces or missing toolpaths must be solved before a final model can be printed. The printed model will be tested to confirm the viability of the design. We thank our Client Stratasys and our faculty advisor Dr. Taylor for guiding us in this project.

References

1. "Home – 3DLabPrint," *3DLabPrint* Available: https://3dlabprint.com/.
2. DS Wingsquad and Aerospaced, "Optimization of the Internal Topology and Sizing for Thin-Walled Aircraft Structures. A Design and Production Guideline for Fused Deposition Modeling," May 2018.

3D Printed Aircraft Fuselage

Niakan, B., Horton A., Scarlett, E., Yu, S., Jimenez, A., Harmina, V.
ME Senior Design

UNIVERSITY OF TEXAS ARLINGTON | COLLEGE OF ENGINEERING

Executive Summary

The purpose of the 3D Printed Aircraft Fuselage project is to successfully 3D print a scaled down aircraft fuselage with a structural design that can withstand applied aerodynamic loads. This project has been worked on by multiple design groups throughout the past few years. However, major printing failures, such as bead layer overlapping and contoured surface bonding failures, have prevented these groups from successfully 3D printing a structurally sound fuselage. These problems were also enhanced by an overly complex structural topology design. This team took on the task of directly solving these major issues, and any more that may arise, through topology optimization, design simplification, rough model creation, model refinement, structural analysis, and test printing. Once the fuselage is successfully printed with sound structural integrity, it will be tested with the applied loads. If the fuselage withstands the applied loads, the goal of the project will be complete.

Background

3D printing makes parts by depositing beads of material on a horizontal plate which then fuse together. As the material for the part proceeds in the vertical direction, the plate moves down so the next layer can be deposited on the preceding layer of material.

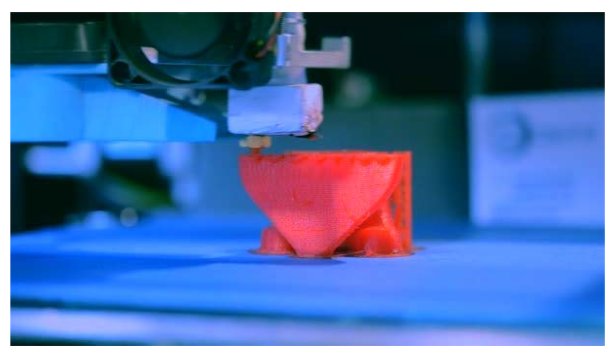

Figure 1. FDM 3D Printing Part

There are many benefits to 3D printing such as the lower time it takes to make a part, high accuracy, and the ability to verify the design of a part within a smaller time window. Because it takes less time, parts can be tested, redesigned, and reprinted in a short period of time. This capability makes 3D printing an ideal process to rapidly manufacture prototypes and models for various applications. In the case of this project, we are 3D printing a model aircraft fuselage, with interior supports, to give insight into how a complex part model can designed to be rapidly 3D printed.

Conceptual Design Phase

The base aircraft model to be used in the project was researched and selected, by the previous design group, from OpenVSP (Fig. 2).

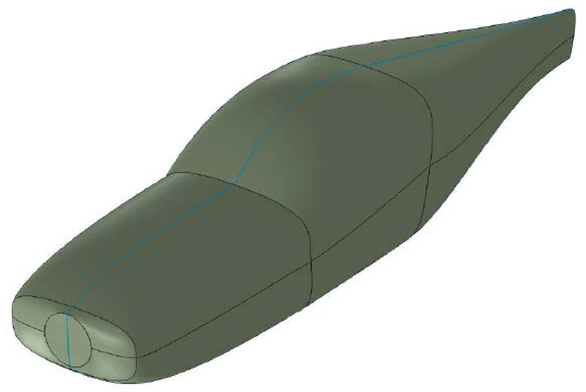

Figure 2. Base Fuselage Model

This model would be hollowed out to print as a shell with one print bead skin thickness with interior structural supports, or stiffeners. These stiffeners would act as members that protrude inward from the skin to transfer the loads throughout themselves, and not the fuselage skin.

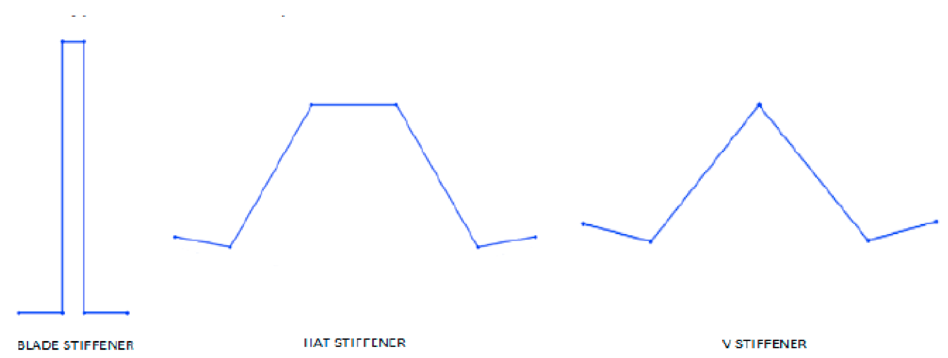

Figure 3. Stiffener Cross-Sections

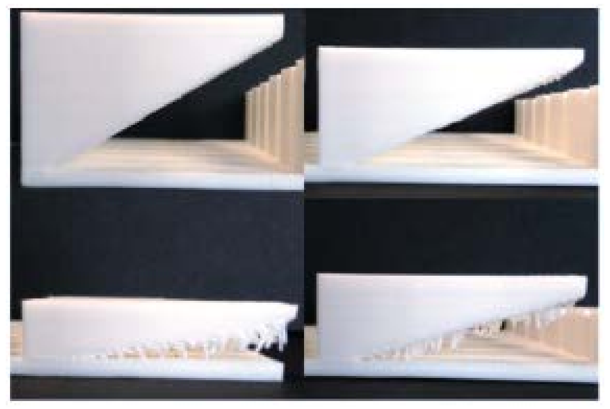

Figure 4. Failed Prints

Detailed Design Phase

The optimum layout of stiffeners was computed using topology optimization in HyperWorks (Fig. 5).

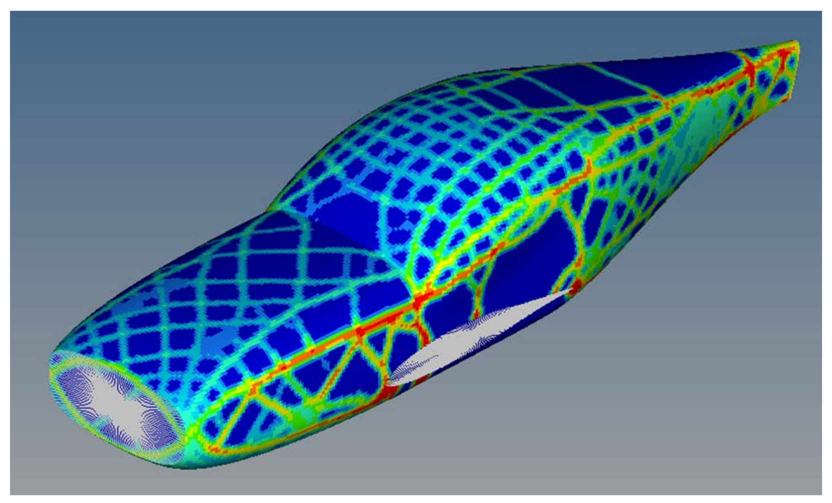

Figure 5. Optimization Results

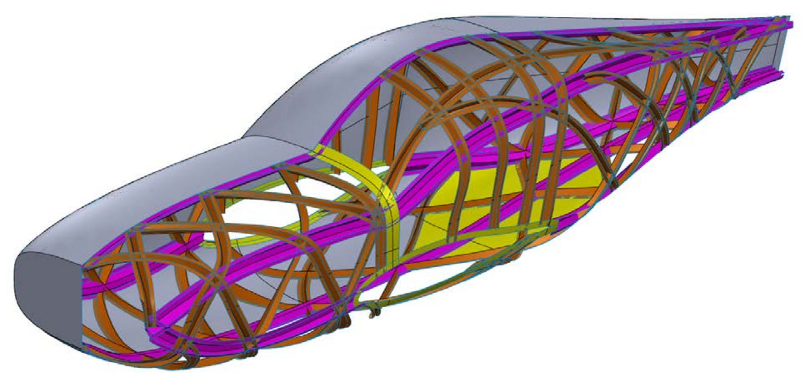

Figure 6. Whole Stiffener Model

The optimization results were used as a bases for the stiffener design, while still carefully considering surface printability. The fuselage was then cut into three pieces to be printed separately, due to print height limitations. Joints for each piece were modeled based on a design from the previous design group.

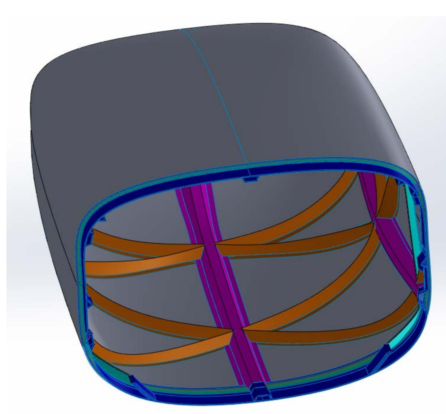

Figure 7. Nose

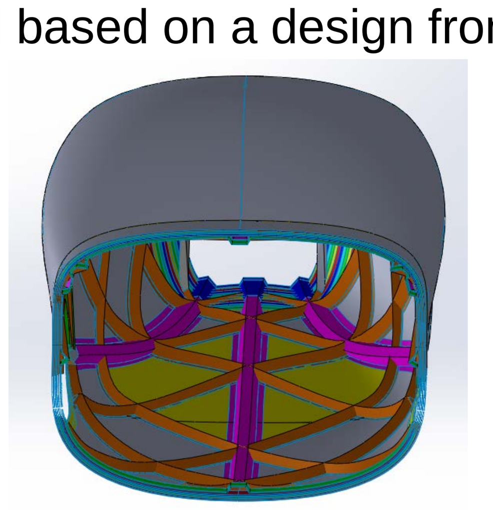

Figure 8. Middle

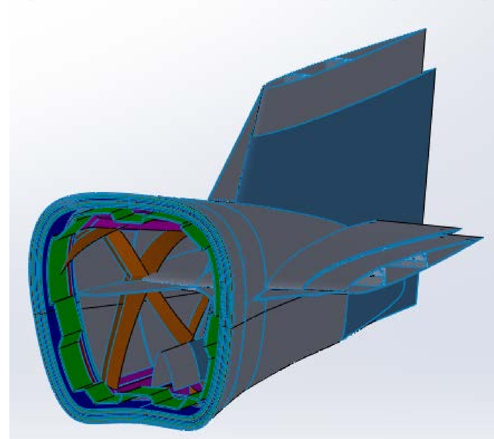

Figure 9. Tail

Prototype & Test

Various test pieces were printed by this design group and previous design groups that gave important insight into how certain designs of the fuselage would print.

Figure 10. Female Joint Test Piece

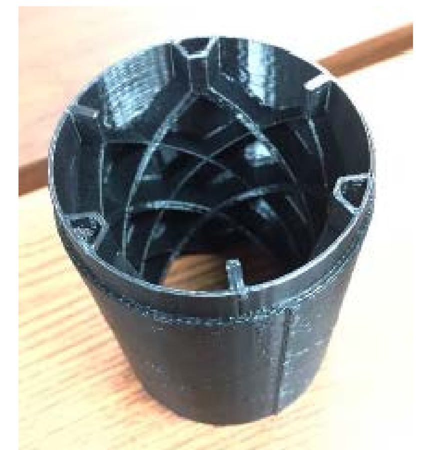

Figure 11. Male Joint Test Piece

Test prints from previous years also gave this group insight into designs that failed, and would be carefully analyzed.

Figure 12. Failed Stiffener Test

Figure 13. Bulging Material Failure

Conclusions

Thanks to progress made by previous design groups working on this project and assistance given by our faculty sponsor, Dr. Taylor, this design group was able to redesign a 3D printed model aircraft fuselage to ensure improved printability. However, final printability adjustments must still be made before the fuselage can be fully printed. While the significant problems, such as overlapping material and failed stiffener orientations, have been largely solved in the CAD model of the fuselage, a print of a full section is still pending to determine how effectively these problems were solved. There are some adjustments to the project that could be made in the future, such as a joint system that better transfers loads across sections or how to develop a more accurate stress analysis of the fuselage.

References

1. UT Arlington "DS Wingsquad" & Aerospaced (2018). Optimization of the Internal Topology and Sizing for Thin-Walled Aircraft Structures–A Design and Production Guideline for Fused Deposition Modeling. University of Texas at Arlington.
2. The Concise Guide To Nastran Rigid Elements. Endurasim Pty Ltd., 2008, http://www.endurasim.com.au/wp-content/uploads/2015/02/EnDuraSim-Rigid-Elements.pdf. Accessed 27 Nov 2018.
3. DTU Mechanical Engineering. A Simlified General Work Diagram For TopOpt.. https://www.sintef.no/contentassets/ec0e7d544b83407f93a1f3e6bdb7de96/zeidan_applied-topology-optimization.pdf. Accessed 27 Nov 2018.
4. Indovance. Solid Modeling Versus Surface Modeling. Deshmukh Mandar. 18 Feb 2016, https://www.indovance.com/knowledge-center/info/solid-modeling-versus-surface-modeling/
5. Chalmers University of Technology. Methodology for Topology and Shape Optimization: Application to a Rear Lower Control Arm. Robin Larsson. 2016. https://www.chalmers.se/SiteCollectionDocuments/

2019 UTA College of Engineering Innovation Day **April 15, 2019**

Wheelchair Attachable Modular Assistive Robotic Arm

Team: Alba, Chapin, Jackson, Kubicek, Stallings, Trollinger
Faculty Advisor: Dr. Panos Shiakolas
Mechanical Engineering Senior Design

UNIVERSITY OF TEXAS ARLINGTON | COLLEGE OF ENGINEERING

Executive Summary

Dr. Shiakolas has tasked the Assistive Robotic Machines (ARMS) team with creating a modular robotic arm that will serve as the basis for future research in mobility solutions. The main focus of the work done by ARMS is to produce a robotic arm, attached to an electric wheelchair, that is capable of reaching two feet to retrieve a two pound object. When designing the arm, emphasis was placed on keeping the parts as cost effective as possible. Cost was kept low by minimizing organic shapes and by using standard stock dimensions for link tubing. Another design goal was to make the arm modular such that it could be assembled and disassembled by a caregiver. This was accomplished by the use of button clips. Our final deliverable will allow future research groups to develop various forms of end effectors, input devices, and object detection systems.

Background

An estimated 58,000 individuals in the United States alone require assistance with eating and drinking [1]. Existing robotic arms that attach to wheelchairs that would alleviate this dependence start at $26,000 [2]. The end effector alone for these robotic arms costs around $5,000 [2]. After the other hefty financial burdens incurred by a person with a disability, the shear cost of existing assistive technology renders it unobtainable. Without assistive technology, persons with a disability are completely dependent on another person. ARMS interviewed a person with a disability who said that they would be willing to spend as much as $1,500 on a device that would simply retrieve a water bottle from a table. Therefore, $1,500 is the target cost for the prototype created by ARMS. Currently, there are no products on the commercial market that meet our objectives for our target cost. For this reason, ARMS aims to design a cost effective mobility solution to reach as many people as possible.

Conceptual Design Phase

There are 5 common robot arm configurations, as shown in Figure 1. The translating bar on top of the Cylindrical, Cartesian, and Polar arms would pose a risk of injuring the user if it were mounted to a wheelchair. SCARA models are typically fixed in the vertical, or z direction, which is impractical for our application. The jointed, or articulated, design allows for the highest dexterity within the workspace, is the design established by industry precedent, and functions most like an actual human arm. Therefore, this was the design chosen for our application.

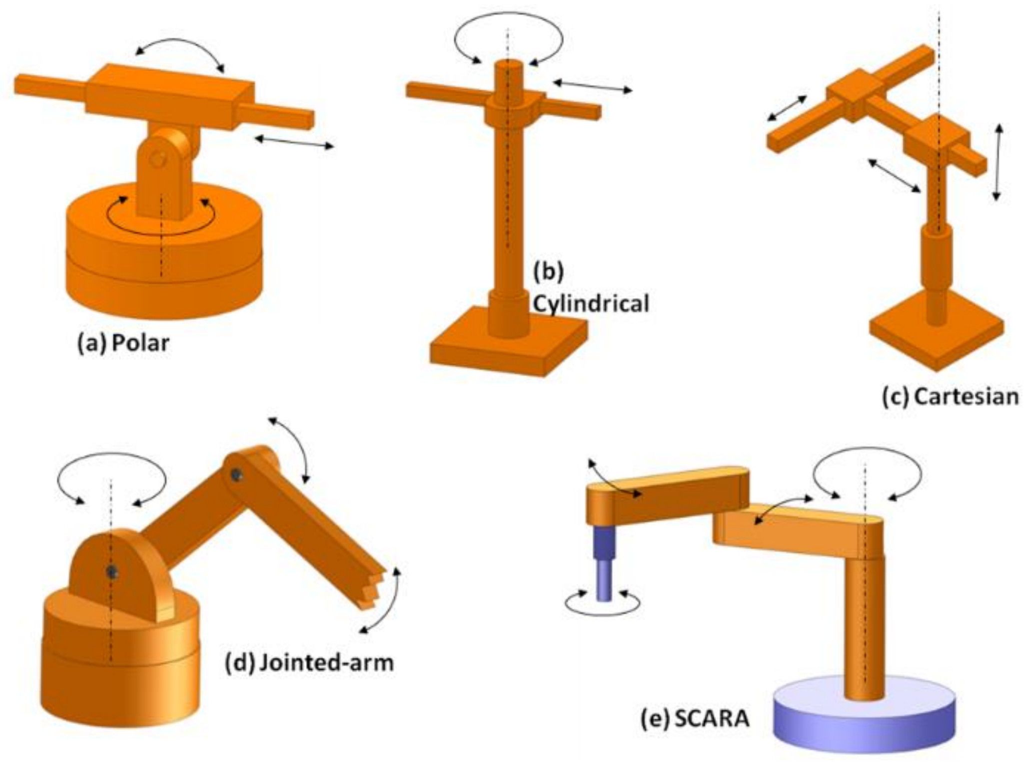

Figure 1. Types of Robotic Arm Designs [3]

Detailed Design Phase

Once the main structure of the robotic arm was determined, the remaining ambiguity was in the joint design. Four concept sketches were drawn, shown in Figs. 2-5. The direct shaft, revolute joint design allows for the largest range of motion and the most cost effective motors. Therefore, the design shown in Figure 2 was chosen.

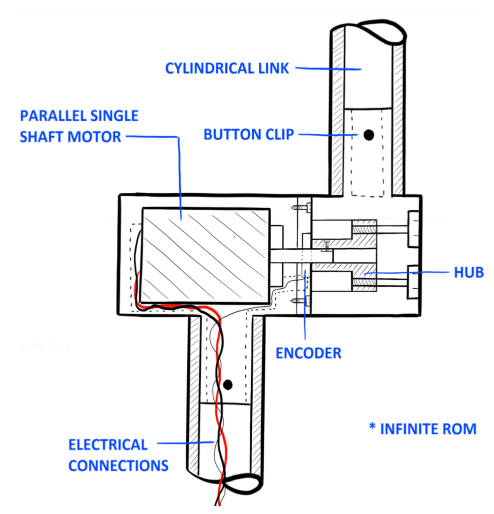

Figure 2. Direct Shaft, Revolute

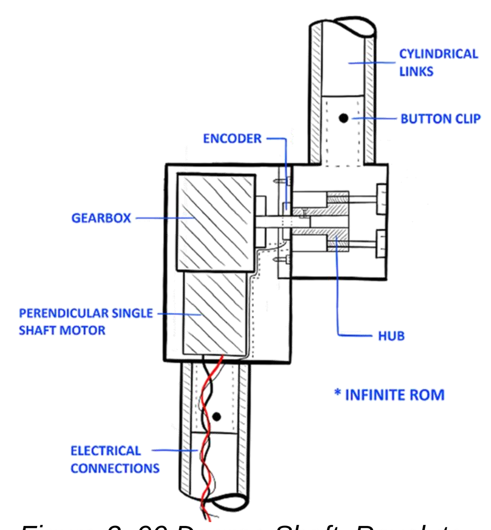

Figure 3. 90 Degree Shaft, Revolute

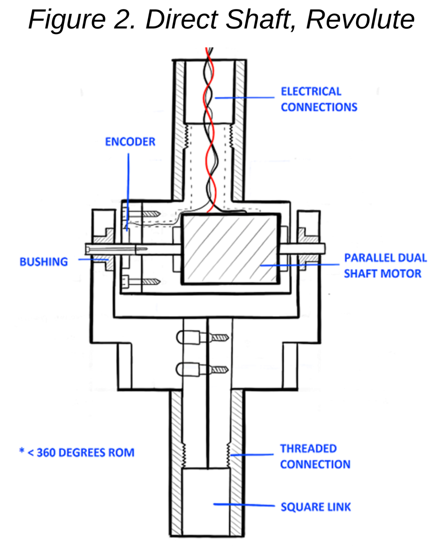

Figure 3. Direct Shaft, Saddle Joint

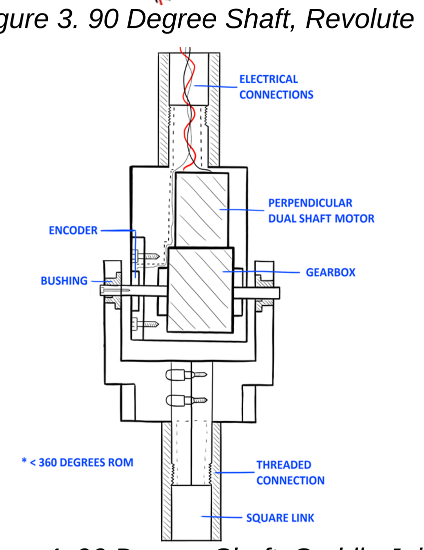

Figure 4. 90 Degree Shaft, Saddle Joint

Prototype

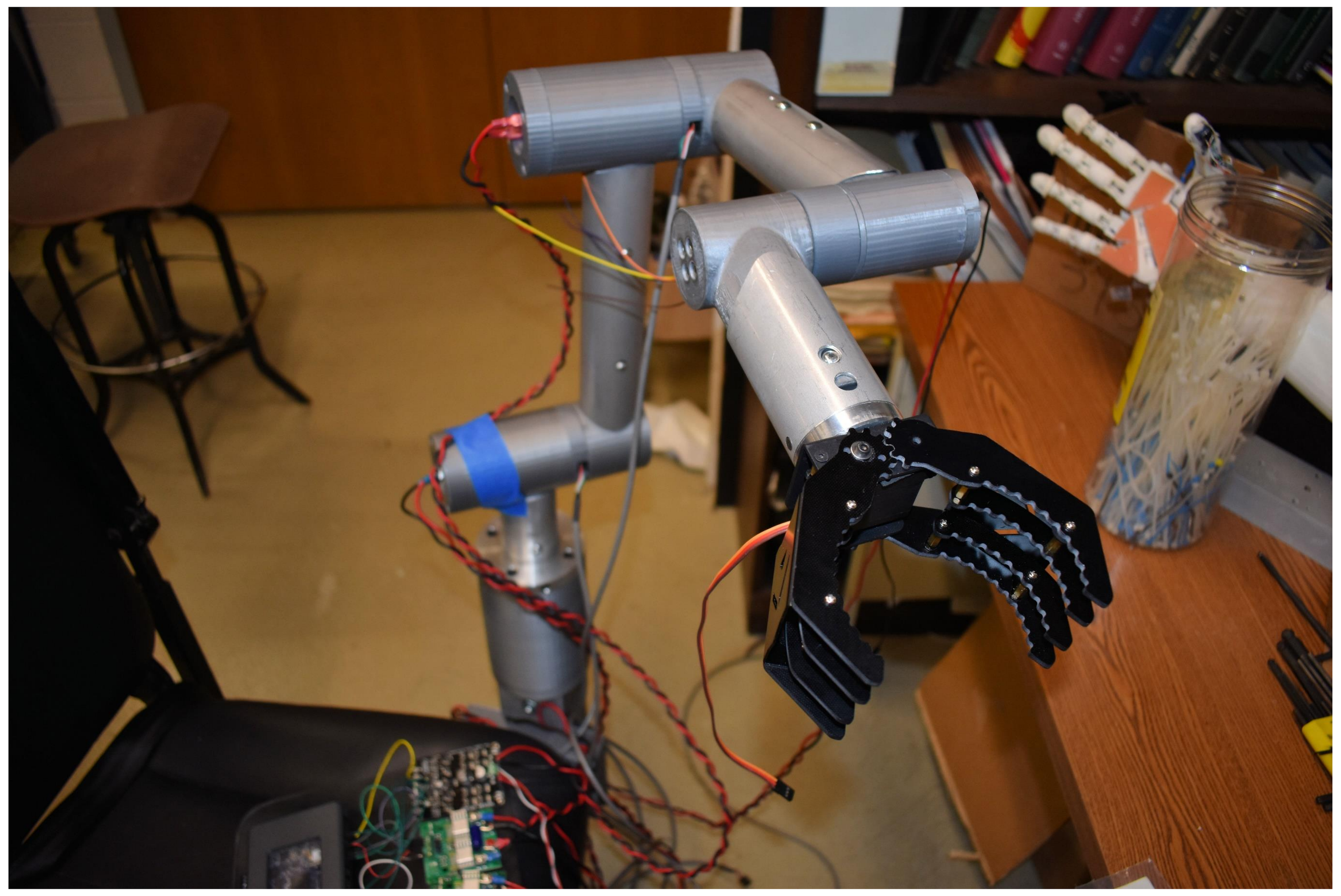

Conclusions

ARMS has successfully created a prototype capable of reaching 2 feet to retrieve a 2 pound object. Even though structural analysis was preformed at every joint to select appropriate motors, the middle joint was not supporting the weight of the arm when first assembled. This joint had to be upgraded to a larger motor. In addition to this, many issues arose after the arm was put together that could not be predicted digitally. Through this process, we learned the importance of designing with manufacturing in mind, that a digital analysis is sometimes misleading, and how to engineer a solution to a complex problem. We would like to thank our REU sponsors and MetroCare Medical for their donations and Dr. Shiakolas for his guidance.

References

1. "Feeding Assistance a Case Study" [ONLINE]. Available: http://www.ewh.ieee.org/soc/es/Aug1996/030/cd/feeding/report/s1.htm [Accessed: 15-Nov-2018]
2. Cobotsguide, "cobotsguide," CobotsGuide, 01-Mar-2018. [Online]. Available: https://cobotsguide.com/2016/06/kinova/. [Accessed: 01-Dec-2018].
3. "Lecture 5 : Industrial robotics-1," Module 7 : CNC Programming and Industrial Robotics. [Online]. Available: https://nptel.ac.in/courses/112103174/module7/lec5/3.html. [Accessed: 01-Dec-2018].

Continuously Variable Displacement (CVD) Engine

Fredrickson, J., Glidewell, E., Goller, R., Hymel, P., Paradis, M., Riley, T.
Mechanical Engineering Senior Design

Executive Summary

Dr. Robert Knezik and Ameriband, LLC came up with an industry changing idea – an engine capable of continuously adjusting its displacement so that it can have the fuel economy benefits of a small displacement engine, while still having the same capability for higher horsepower when adjusted to a large displacement. Our Senior Design team initially worked to compare the frictional losses within the CVD engine and to compare them to that of a traditional engine. A frictional analysis of traditional combustion engines was completed as a benchmark and small advances were made into deriving equations to theoretically estimate the frictional losses in the CVD engine. Following that, a series of smaller issues were addressed, such as bearing selection, along with moving to finalize the CAD design of the engine to meet customer specifications.

Background

Cylinder deactivation is used in traditional engines to increase efficiency, but at the expense of power lost due to friction. The CVD engine is a revolutionary design that varies the cylinder displacement while maintaining a constant compression ratio such that frictional losses are minimized and efficiency is conserved.

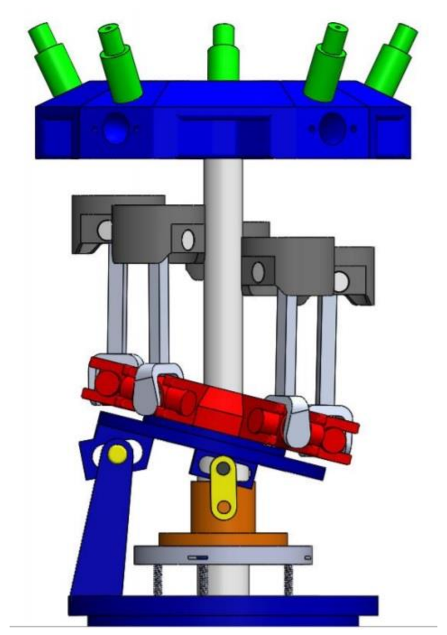

Figure 1. CVD Engine Assembly

Conceptual Design Phase

The original model needed modification to make the CVD engine fully function, which is a critical task fulfilled by our Senior Design team. Additional designs would need to be implemented to realize the goals of the CVD engine while maintaining functional ability.

Table 1. Design Requirements

Item	Requirement	Solution
1	Bearing Selection	Thrust, ball and socket
2	Centering the UWP	CV Joint
3	Increase Fatigue Life of Connecting Rod	Circular Cross Section
4	Control Vertical Translation of PTU	Model an Anchor
5	Engine Housing	Split Housing with Journal Bearing for Power Shaft

Detailed Design Phase

A Timkin Type TVL Angular Thrust Contact Bearing was selected to withstand misalignment between the Upper Wobble Plate (UWP) and the Lower Wobble Plate (LWP) while undergoing angular and rotational loading (Fig. 1). To keep the wobble plate centered during the engine cycle, a CV joint was designed (Fig. 2). The CV joint required to fit the engine dimensions could not be readily found as a COTS part (commercial off-the-shelf) and had to be modelled. The connecting rod design for the piston is in progress. It will have a circular cross-section to have an infinite fatigue life, as well as to minimize chances of interference between it and the retaining bracket (Fig. 3) when it completes a 30 degree sweep angle through the engine cycle. The Power Transmission Unit (PTU) sits on a lift mechanism and must translate 1.736 in vertically (Fig. 4). The engine housing was designed as a component that could be split for ease of maintenance. It is symmetrical to simplify manufacturing and can accommodate the power transmission shaft, for which a journal bearing will be used at the point of contact (Fig. 5). The complete model should neatly package all of the engine components (Fig 6.)

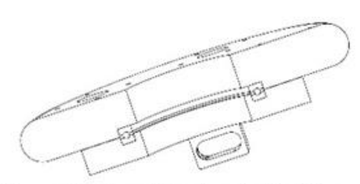

Figure 1. Thrust Bearing in Position

Figure 2. CV Joint

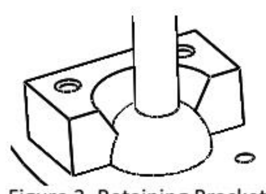

Figure 3. Retaining Bracket

Figure 4. PTU

Figure 5. Split Engine Housing

Figure 6. Complete Engine Case

Prototype & Test

The majority of our testing has occurred via ANSYS. Parts have been tested to ensure they will endure the forces and stresses that an internal combustion engine undergoes. The connecting rods are still undergoing design iterations and will need to undergo a buckling analysis, but that will need to be done via MATLAB, since the ANSYS buckling test is unreliable. Multiple small scale calculations are also being performed to calculate forces at various stages of the combustion cycle, along with the hydraulic pressure that will be required to maintain the position of the wobble plate actuators.

Conclusions

Our client has guided us through this process quite thoroughly, so our team is confident that we will give the client a product that matches the specifications and performs the task that they want. The CAD models and engineering drawings that we turn over at the conclusion of this project should allow the client to 3D print a 1:1 scale model, which will help them to work out the final kinks in the design before they invest in a working prototype.

There are many things that we have collectively learned throughout this project, and we owe a great deal of gratitude to Dr. Robert Woods and Dr. Robert Knezik for helping to guide us through this challenging project.

References

1. Dynamic Solutions, "Knezek Axial Engine," Senior Design Final Report, Department of Mechanical and Aerospace Engineering, University of Texas at Arlington, Arlington, Texas, 2018
2. Essay UK, "Distribution of Friction Losses in I.C. Engine," Essay UK, http://www.essay.uk.com/free-essays/engineering/distrinution-friction-losses.php
3. Subbarao, PMV, "Mechanical Losses in an Engine," Mechanical Engineering Department, Indian Institute of Technology Dehli, Hauz Khas, New Delhi, India, 2012

Student Design Competition ASHRAE 2019

By Summit Group : Cornell, Sherpa, Soto, Saroj, Andino .

ME Senior Design

UNIVERSITY OF TEXAS ARLINGTON | COLLEGE OF ENGINEERING

Executive Summary

The Summit Group's aim is to calculate the heating and cooling loads for a four-story hospital building located in Budapest, Hungary, and then to select the most appropriate HVAC system for the hospital. The primary focus of this process is meeting the specific owner project requirements (OPR), while also complying with ASHRAE standards. Some of those requirements include system sustainability, energy efficiency and safety, occupant comfort and functionality, longevity and flexibility, serviceability and maintainability.

The Summit Group identified building zones for which heating and cooling loads have been calculated for each floor. Subsequently the team selected equipment for each system option and conducted life-cycle cost analyses to narrow the field of possible choices down to the proposed system. The team selections emphasized high performance, as well as the comfort and design sophistication necessary to minimize the risk of airborne pathogen transmission and preserve a sterile healing environment for patients and staff.

The Summit Group design analysis process:

- Provides heat and cooling load estimates
- Incorporates the sustainability process by integrating ASHRAE standards
- Ensures reasonable life-cycle costs
- Yields a system design within the allowable budget

Trace 3-D Plus

Trace 3D Plus
Energy plus platform

- Integrated, simultaneous solution
- Sub-hourly, user definable time steps
- Weather input and output files
- Combined heat and mass transfer
- Thermal comfort models
- Loop based configurable HVAC systems

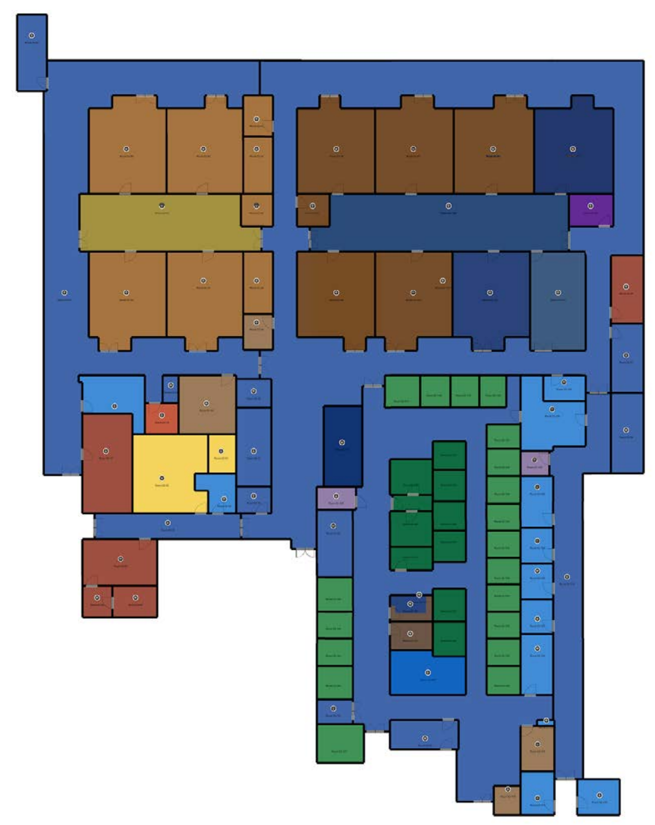

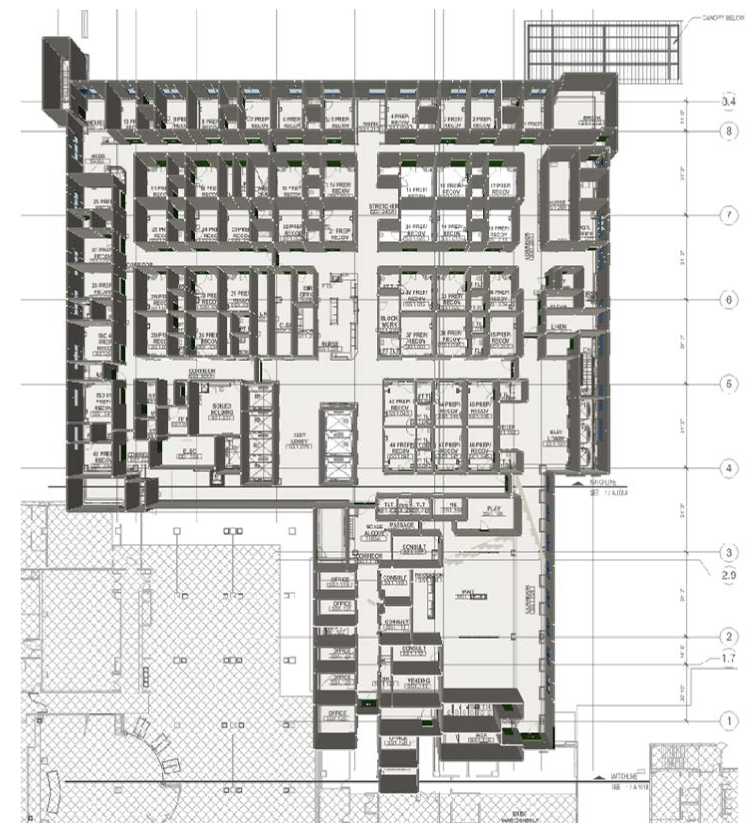

Cost & Financial Estimation

The projected costs of the two systems in consideration are analyzed for a lifespan of 50 years. the first system in consideration is a VAV unit with a Water Chiller plant, and the second unit is a VAV with an Air Chiller plant.
From the cost estimation, the VAV Air Chiller sees more operating costs over 50 years than the VAV Water Chiller. Maintenance costs for both systems is roughly the same, while water chiller replacement costs are less than air chiller costs. In told, the Water chiller sees less utilities cost, less maintenance & operating costs, and lower initial costs than the Air Chiller equivalent.

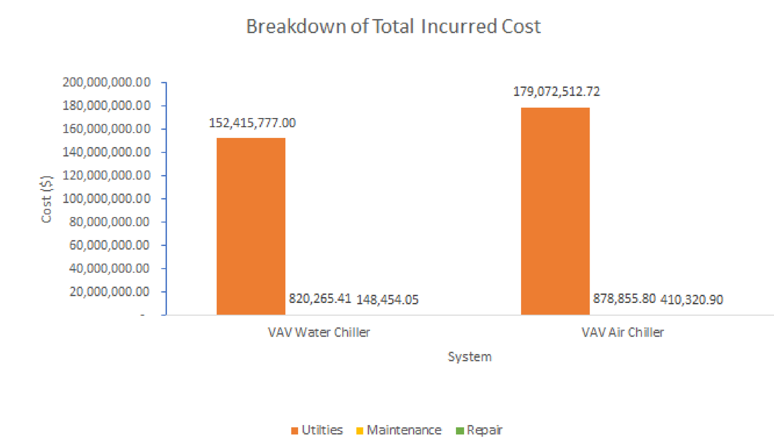

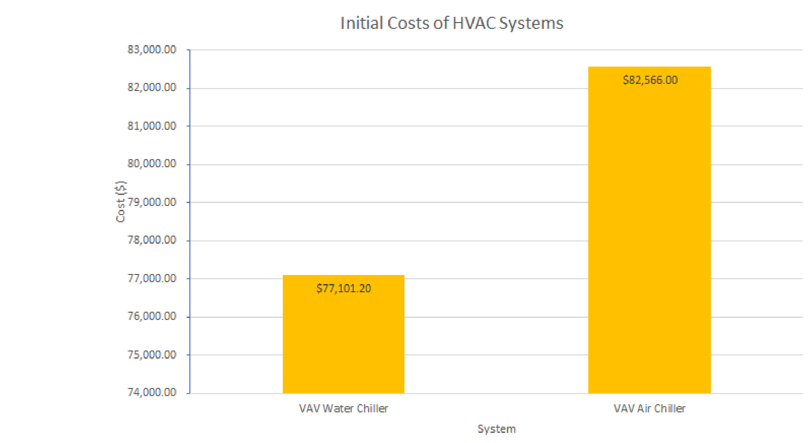

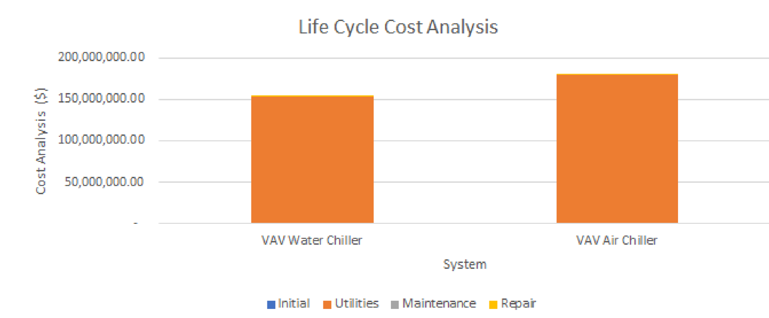

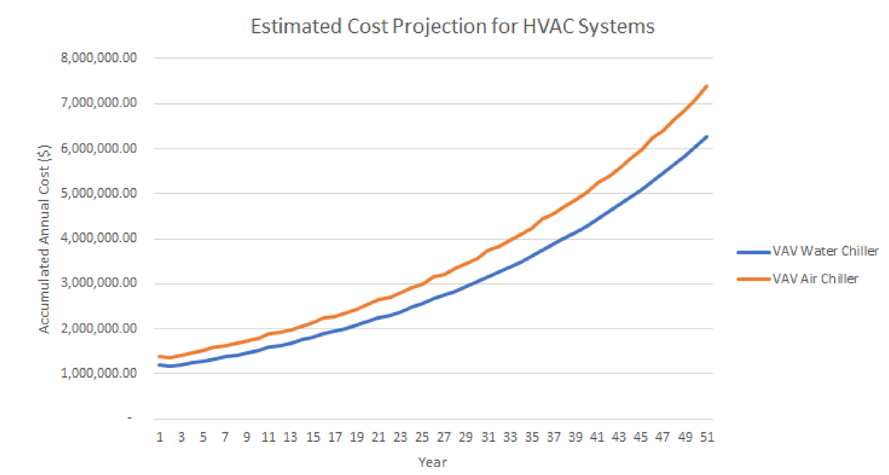

Background

This project requires the design of a heating, ventilating and air conditioning system for a four-story medical complex with a building area of 70,000 square feet in Budapest, Hungary. The facility's primary features include surgical operating rooms, office spaces, laboratories, shared spaces such as reception areas, conference rooms, storage, and a data center. The objective of the project is to design a sustainable system with low life-cycle cost, low environmental impact, optimum occupant comfort and health, and a high-performance green design. Load calculation is a crucial part of the HVAC design in which cooling and heating loads for the system are calculated. The HVAC system's components and equipment are selected based upon the accurate determination of cooling and heating loads.

ASHRAE Standards

- ❖ 90.1
Determination of Energy Savings: Quantitative Analysis
- ❖ 55
Thermal Environmental Conditions for Human Occupancy
- ❖ 62
Ventilation for Acceptable Indoor Air Quality
- ❖ 107
Ventilation of Health Care Facilities
- ❖ 189.1
Design of High-Performance Green Buildings Except Low-Rise Residential Buildings
- ❖ Energy Considerations

System Performance

Temperature Profile and Humidity Profile

The temperature and humidity profile of the various conditioned zone of the building.

Zone Name	Unmet Heating Hours	Minimum Temperature (°F)	< 50°F	50°F ≤ 55.4°F	55.4°F ≤ 60.8°F	60.8°F ≤ 66.2°F	66.2°F ≤ 71.6°F	71.6°F ≤ 77°F	77°F ≤ 82.4°F	82.4°F ≤ 87.8°F	87.8°F ≤ 93.2°F	93.2°F ≤ 98.6°F	> 98.6°F	Unmet Cooling Hours	Maximum Temperature (°F)	Mean Temperature (°F)
			Time spent in each temperature range (°F)													
Admin 1	0	70					8687	73						0	72	70.1
Admin 2	0	70					8742	18						0	72	70
Admin 3	0	70					7134	1626						28	73.2	70.6
Admistrative	0	68					8678	82						0	73	70
Corridor 1	0	70					8760							0	70.7	70
Corridor 2	0	70					8760							0	71.1	70
Corridor 3	0	70					8751	9						0	72.4	70
costodial	0	69.9					8469	291						0	73.4	70.2
Isolated-Corridor	0	68					8760							0	70	69.4
Lab	0	70					8760							0	71.4	70
Mechanical	0	70					8760							0	70.1	70
Mechanical 1	0	70					5347	3413						0	72	70.9
Mechanical 2	0	70					8760							0	70.4	70
Mechanical 3	0	78.6							8760					0	78.6	78.6
Operating room	0	60			451	8309								15	64.3	61.9
Patient room	0	70					8745	15						0	72.4	70
Patientroom 1	0	70					8760							0	70.5	70
Residential	0	70					8760							0	70.1	70
Restroom 0	0	69.9					8742	18						0	72	70
Restroom 1	0	68					8505	255						0	73	69.7
Restroom 2	0	70					5115	3645						0	72	70.9
Restroom 3	0	70					8756	4						0	72	70
Stairway/Corridor	0	68					8760							0	70.9	69.5
Strelization	0	68					8760							0	70.8	69.5
Strelization 1	0	70					8760							0	70.6	70
Strelization 2	0	70					8754	6						0	72	70

Zone Name	Minimum % Relative Humidity	< 30%	30% ≤ 35%	35% ≤ 40%	40% ≤ 45%	45% ≤ 50%	50% ≤ 55%	55% ≤ 60%	60% ≤ 65%	65% ≤ 70%	70% ≤ 75%	75% ≤ 80%	> 80%	Maximum % Relative Humidity	Mean % Relative Humidity
Admin 1	43.5	0	0		32	334	2757	2158	2542	935	2			70.7	58.1
Admin 2	42.1	0	0		117	2744	4341	1523	35					63.2	51.9
Admin 3	45.9	0	0			83	1568	4594	1842	531	142			74.4	58.6
Admistrative	41.4	0	0		88	721	3030	2231	2484	204	2			70.6	56.3
Corridor 1	41.1	0	0		125	1058	5318	1795	456	8				66	53.4
Corridor 2	39.6	0	0	30	274	4557	3324	568	8					60.7	49.9
Corridor 3	42.6	0	0		55	183	3796	4301	425					64.8	55.3
costodial	18.8	8760												28	24
Isolated-Corridor	39.9	0	0	3	190	3289	4394	840	43	1				65.8	50.9
Lab	43.4	0	0		45	996	5142	2509	68					64.2	53.1
Mechanical	49	0	0			49	188	2594	4108	1601	204	16		77	62.1
Mechanical 1	41.2	0	0		86	1824	5651	1135	64					64.5	52
Mechanical 2	41.6	0	0		161	3425	4572	594	8					60.8	50.8
Mechanical 3	32.8	0	99	1986	6565	111								47.7	41.2
Operating room	57.4	0	0					95	1770	5292	1548	51	4	83.9	67.4
Patient room	43.9	0	0		32	1080	6259	1361	28					64	52.8
Patientroom 1	49.2	0	0			22	483	3371	4319	553	12			72.6	60.3
Residential	42	0	0		92	223	5209	2321	884	32				67.3	55.1
Restroom 0	7.4	8760												11.6	9.1
Restroom 1	28.4	76	5905	2776	4									40.7	34.4
Restroom 2	39.3	0	0	5	756	5859	2112	25	3					61.4	48.6
Restroom 3	44.3	0	0		27	142	1993	5656	930	13				66.1	56.5
Stairway/Corridor	49.3	0	0			16	113	908	4675	2105	834	102	8	82.5	64.5
Strelization	50.5	0	0				87	698	3760	3219	938	50	8	82.6	65.1
Strelization 1	29.1	41	2727	5779	214									43.4	36.1
Strelization 2	45.4	0	0			321	3148	4737	545	9				66.5	55.7

VAV-Air Cooled Chiller

Zone Name	Unmet Heating Hours	Minimum Temperature (°F)	< 50°F	50°F ≤ 55.4°F	55.4°F ≤ 60.8°F	60.8°F ≤ 66.2°F	66.2°F ≤ 71.6°F	71.6°F ≤ 77°F	77°F ≤ 82.4°F	82.4°F ≤ 87.8°F	87.8°F ≤ 93.2°F	93.2°F ≤ 98.6°F	> 98.6°F	Unmet Cooling Hours	Maximum Temperature (°F)	Mean Temperature (°F)
			Time spent in each temperature range (°F)													
Admind-level 2	0	68					8750	10						0	72.4	69.5
Admin-level 1	0	68					8668	92						0	73.4	70
Admistrativ level 3	0	68.9					8282	478						0	73.4	70.1
Admistrative level 0	0	68					8760							0	71.5	69.9
Corrider-01	0	65				1955	6805							0	70	68.6
Corridor-02	0	70					8760							0	70	70
Corridor-Level 0	0	65				1936	6824							0	70	68.6
costodial-01	0	69.9					8747	13						0	72.3	70
Isolated-Corridor-02	0	64.9				5692	3068							0	70.4	65.9
IT server-02	0	78.6							8760					0	80.7	80.1
Lab-02	0	70					8760							0	70.1	70
Mechanical-0	0	60			3635	5125								0	65.6	61.5
Mech-level 3	0	60			2218	4948	1566	28						0	73.6	63.4
Operating room-02	0	60			438	8322								0	62	61.9
Patient room-01	0	70					8760							0	70.6	70.1
Patient-02	0	70					8760							0	71	70
Residential-03	0	70					8760							0	70	70
Restroom-03	0	70					8328	432						0	73.4	70.2
Restroom-Level 0	0	65				1448	7312							0	70	68.8
Restroom-Level 1	0	65				775	7985							0	70.4	68.8
Stairway/Corridor-03	0	68.9					8760							0	70	70
SteriliZation-level 0	0	65				1966	6794							0	70	68.6
Strelization-03	0	70					8760							0	71.4	70
StreliZation-level 1	0	69.9					8760							0	70	70
Zone _ITserver_level_1	0	82.7								8760				0	83.2	82.7
Zone 00_IT server	0	82.6								8760				0	82.6	82.6

Zone Name	Minimum % Relative Humidity	< 30%	30% ≤ 35%	35% ≤ 40%	40% ≤ 45%	45% ≤ 50%	50% ≤ 55%	55% ≤ 60%	60% ≤ 65%	65% ≤ 70%	70% ≤ 75%	75% ≤ 80%	> 80%	Maximum % Relative Humidity	Mean % Relative Humidity
Admind-level 2	36.3	0	0	3	6	4085	3789	832	44	1				65.5	50.7
Admin-level 1	45.7	0	0			1463	3073	1303	2508	394	10	3	7	83.1	55.1
Admistrativ level 3	25.6	8	9	19	1625	4697	1583	437	255	128				68	48
Admistrative level 0	40.9	0	0		1700	3279	2731	1042	9					62.1	48.6
Corrider-01	30.7	0	4442	3331	878	99	11							53.9	36.3
Corridor-02	28.3	3	7	6906	1783	61								48.9	39
Corridor-Level 0	40.7	0	0		3006	3567	1487	694	6					63.2	48.2
costodial-01	19.8	8751	10											30.9	22.5
Isolated-Corridor-02	23.1	1827	6528	405										40	31.3
IT server-02	28.2	3	1027	7670	60									43.7	36.5
Lab-02	39.9	0	0	1	6	1247	6832	630	45					63.8	52.1
Mechanical-0	55	0	0					3837	4581	338	4			71.3	60.7
Mech-level 3	31.3	0	3	7	56	1307	2540	4068	780					63.9	55.1
Operating room-02	51.7	0	0				3	5	2356	6120	240	36		79.9	66
Patient room-01	100	0	0										8760	100	100
Patient-02	40.5	0	0		5	448	7767	505	35					63.9	52.1
Residential-03	23.2	10	17	24	5730	2659	283	32						58.7	44.5
Restroom-03	24.1	10	18	20	5718	2933	49	12						57.2	44.8
Restroom-Level 0	40.3	0	0		3028	3900	1577	251	5					61.8	47.7
Restroom-Level 1	8	8760	0											14	8.9
Stairway/Corridor-03	23	15	16	22	6837	1783	77	11						57.2	44
SteriliZation-level 0	41	0	0		2126	3699	2172	753	10					64.3	48.8
Strelization-03	26.7	5	12	19	16	6004	2603	81	20					62.3	48.8
StreliZation-level 1	28.8	1288	7273	164	36									44.3	31.4
Zone _ITserver_level_1	49.3	0	0			31	4452	3463	640	89	38	11	37	100	55.6
Zone 00_IT server	27.4	5903	2857											34	29.9

VAV-Water Cooled Chiller

Conclusions

The proposed 70,000 ft² hospital in Budapest, Hungary must comply with the International Building Code, ASHRAE Handbook - Fundamentals, and ASHRAE Standards 15, 55, 62.1, 90.1, and 189.1, which include standards regarding load criteria, safety, thermal environmental conditions, ventilation for acceptable indoor air quality, energy, and designs for high-performance green buildings. Based on the Trace 3D plus's load calculation simulation, the building would require 1233 MBH of heating, 1500 MBH of cooling, and 94900 cfm outside air to be adequately conditioned. Based on system performance, the VAV System can provide all required air condition for each space type incorporated into the building. Operating costs of the VAV Water Chiller system total less than 154 million dollars in projected inflation, where the VAV Air Chiller system operating costs are set at under 181 million dollars. Despite the increased maintenance costs and relative consistency of power consumption of the VAV system, when accounting for inflation and nominal discount rate its operating cost is less than that of the Chiller system. In total, a VAV Water Chiller system setup for the hospital is 27 million dollars cheaper at the 50 year mark than the VAV Air Chiller system. This sufficiently justifies selection of the VAV Water Chiller system by the Summit Group.

References

2011 ASHRAE Handbook: Applications. American Society of Heating, Refrigeration, and Air Conditioning Engineers, Inc. Atlanta, GA: ASHRAE, 2011. Print.

2013 ASHRAE Handbook: Fundamentals. American Society of Heating, Refrigeration, and Air Conditioning Engineers, Inc. Atlanta, GA: ASHRAE, 2013. Print.

2012 ASHRAE Handbook: Heating, Ventilating, and Air-conditioning Systems and Equipment. American Society of Heating, Refrigeration, and Air Conditioning Engineers, Inc. Atlanta, GA: ASHRAE, 2012.

Print.

2019 UTA College of Engineering Innovation Day April 15, 2019

PTFE Preform Knitting Process Improvement

Anderson, B., Garcia, M., Hong, A., Nguyen, T., Tran, T., Rowlette, J.
ME Senior Design

UNIVERSITY OF TEXAS ARLINGTON | COLLEGE OF ENGINEERING

Executive Summary

The Maverick Manufacturing team was tasked with improving the manufacturing process of polytetrafluoroethylene (PTFE) tubes for Parker Hannifin. Operators perform a process called preform knitting when loading four preforms at a time into a ram extruder. The current process was deemed unsafe and inefficient due to the use of razor blades by hand. The solution was to design and manufacture a prototype, pneumatic cutting mechanism that improves safety and efficiency while also reducing time and labor.

Figure 1. PTFE Tubes

Background

PTFE tubes are used widely in various industries, such as aerospace, medical, and food. Parker Hannifin manufactures these tubes by loading compressed powder of PTFE, formed into the shape of a cylinder known as a preform. They are then inspected by laser calipers to check for outside diameter, elongation, tensile strength, strength at high pressures, and concentricity.

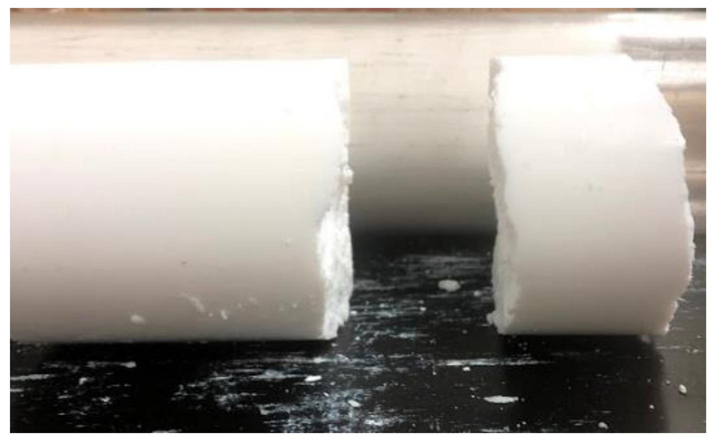

Figure 2. Sample Preform

Conceptual Design Phase

The design requirements for the system are that it needed to be safe, efficient, waste less material, decrease the tubing defects due to the preform knitting process, allow for no contamination, and be backed by experimental data. Initial designs were sketched and reviewed for consideration for the final overall design and accepted designs were modeled in SolidWorks. The basic geometry consisted of a flat base that could hold the preform steady and a housing for a cutting mechanism.

Experimental procedures provided empirical data that proved what blade was going to be used and how much force was needed to cut the material. Results from the force test are shown in Table 1. From these results, a pneumatic actuator was sized by dividing the supply pressure (60 psi) to the force to find the minimum bore.

Table 1. Force Test Results

Run #	Average Force (lbf)
1	11.3 ± 1.38
2	11.4 ± 2.03

Detailed Design Phase

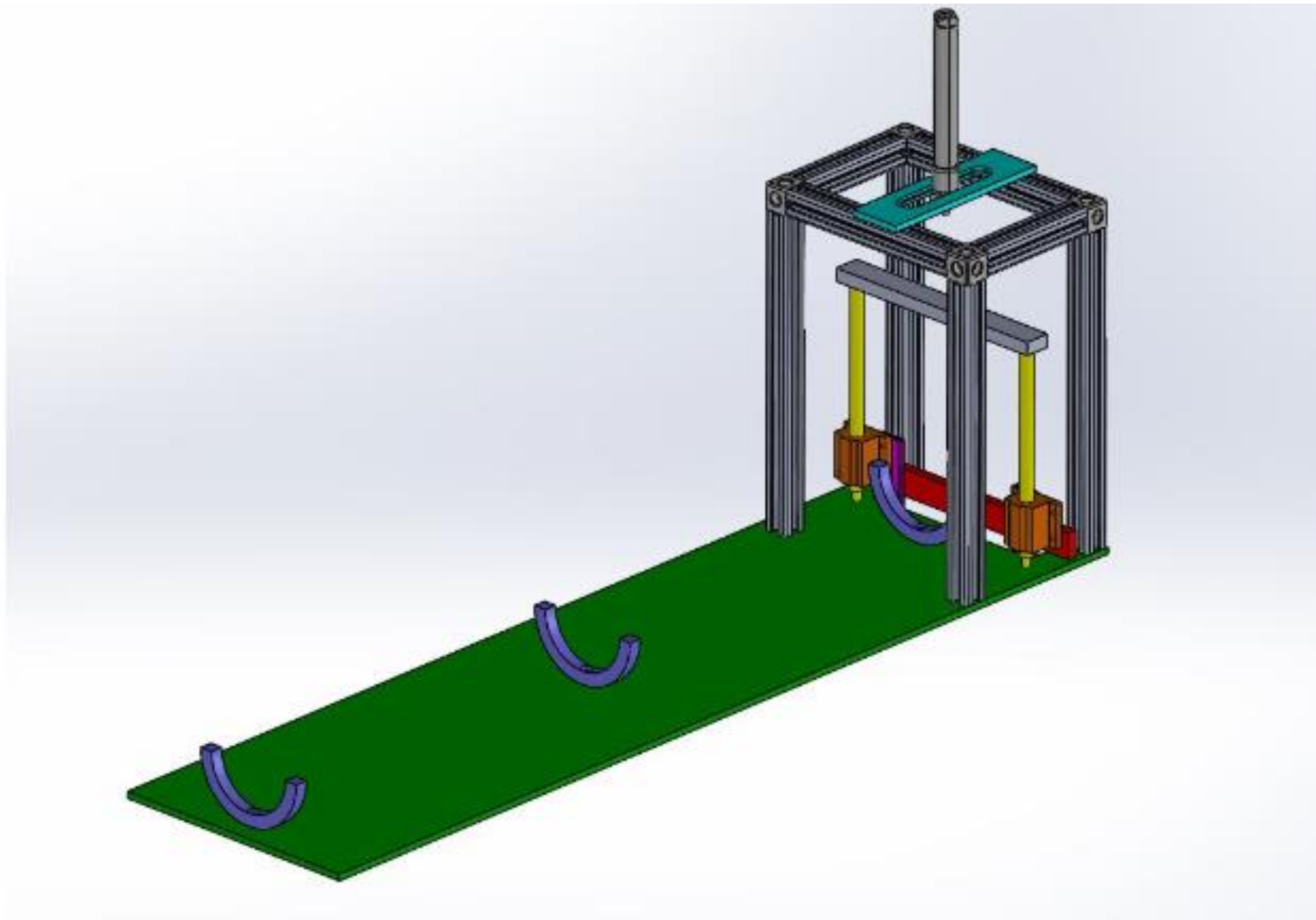

Prototype & Test

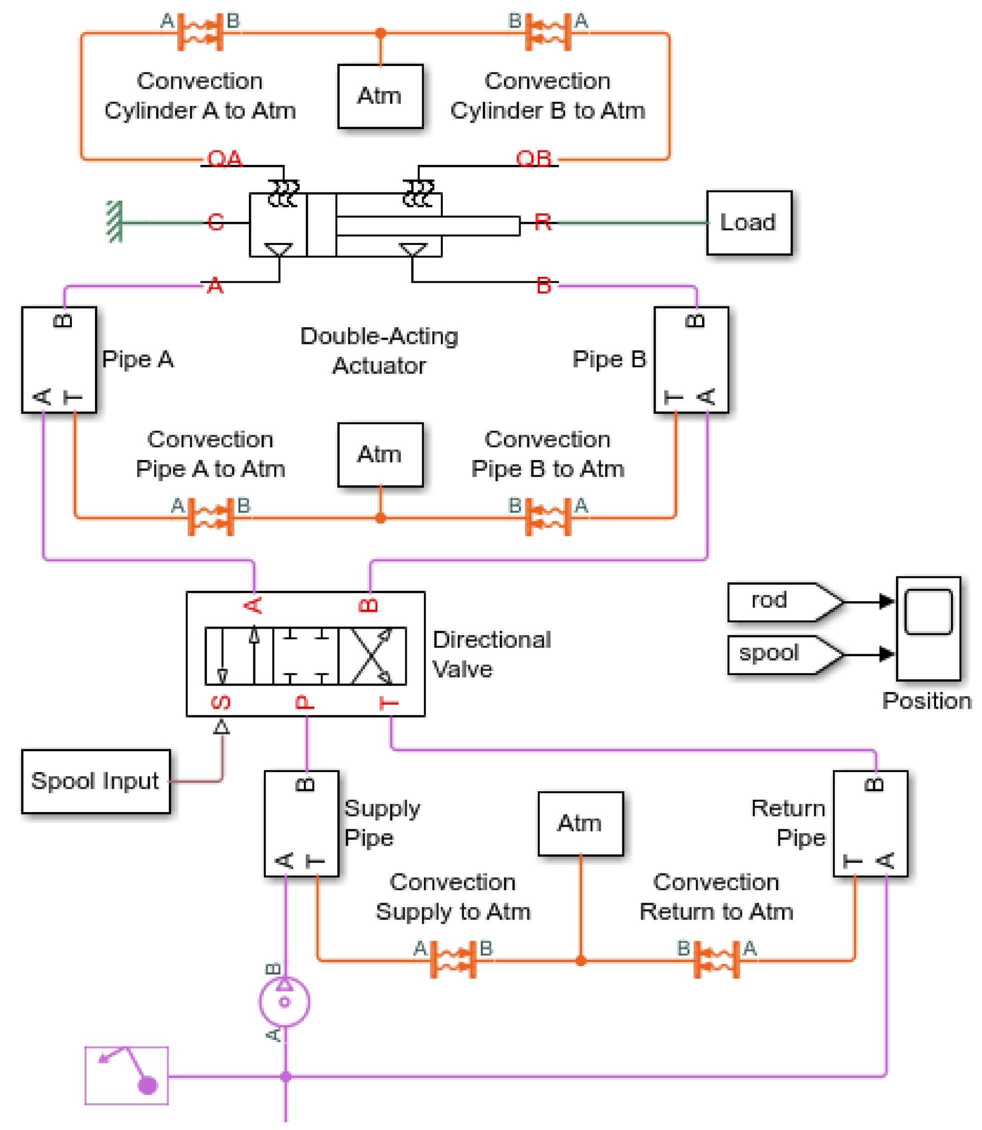

Figure 3. Pneumatic Actuation Circuit (1)

Conclusions

As of April 15th, the system prototype is being manufactured and assembled together, with further trials to make sure the EPK is working as intended. The pneumatic system is working as intended and demonstrated the necessary force to cut the preform. Blade choice and roughing techniques are a concern at the moment since preliminary trials with the prototype show low quality of knitting using the guillotine style. The Maverick Manufacturing team thanks Dr. Raul Fernandez for his guidance during the project and Luke Porter and the machinists of Parker Hannifin for assisting with creation of the system.

References

1. "Pneumatic Actuation Circuit," MathWorks, https://www.mathworks.com/help/physmod/simscape/examples/pneumatic-actuation-circuit.html.

Convolution Spindle

McKenna, W., Brown, C., Patel, M., Anthony, W., Carter, L.
ME Senior Design

UNIVERSITY OF TEXAS ARLINGTON | COLLEGE OF ENGINEERING

Executive Summary

Parker Hannifin has developed an innovative process to manufacture convoluted tubes, but wishes to replace the spindle which holds the smooth-bore tubing and allows for unwinding as it is fed into the extrusion die, which forms the convoluted surface of the tube.

TubeDudes understands that, currently, tubes must be loaded manually on to the spindle using a separate staging area, a process which consumes copious time and presents a safety hazard. For this reason, TubeDudes would like to propose a spindle with a side-loading function to eliminate the need for a staging area. This design will allow the operator to simply open the enclosure, load the tubing, and close the enclosure to complete loading. This design will significantly decrease the loading time and increase safety.

Tube Dudes

Background

Parker Hannifin's current convolution tubing manufacturing process involves uncoiling spools of tubing from a staging area onto a convolution spindle, which then unwinds the spools of tubing about their respective X and Z axes to create torsion and prevent kinking within the extrusion oven. The current system, although operational, has certain drawbacks, such as the process of loading the tubing from the staging area to the spindle can take up to 10 minutes and leaves the tubing exposed during the unwinding process, which creates a safety hazard. Additionally, the staging area is tall and upright, increasing the difficulty of operation for shorter machinists. As a team, our goal is to design a convolution spindle that divides the loading time in half to five minutes, fully encloses the tubing to prevent safety hazards, while remaining user friendly for machinists of all heights.

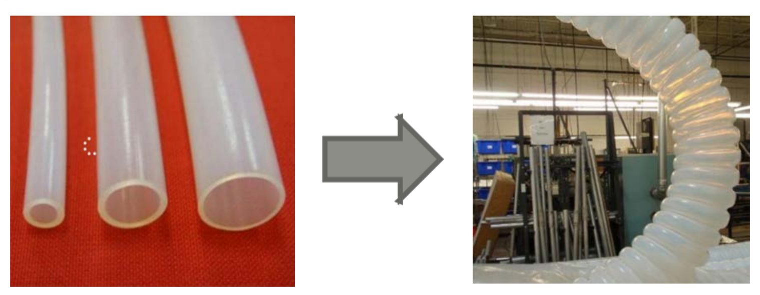

Figure 1. Tubing before and after convolution

Conceptual Design Phase

For the conceptual design phase, we understood that our design would have to remove the need for a staging area to allow for reduced loading time without raising safety concerns. Knowing this, we were able to generate three different conceptual designs: the single beam design, yoke design, or front end loading design. The single beam design reduced the amount of support beams to one on a single side of the wheel, leaving the other side open for the tubing to be loaded. The yoke design consisted of securing the spindle from the top and bottom, tangent to the wheel. The front end loading design left the front edge of the wheel open, which would allow a pre-loaded spool to be fastened into the wheel via a removable shaft. Due to the substantial weight that would accompany the yoke design, and due to the fact that the front end loading design would still technically require a staging area for the pre-loaded spool, we settled with the one beam design going forward.

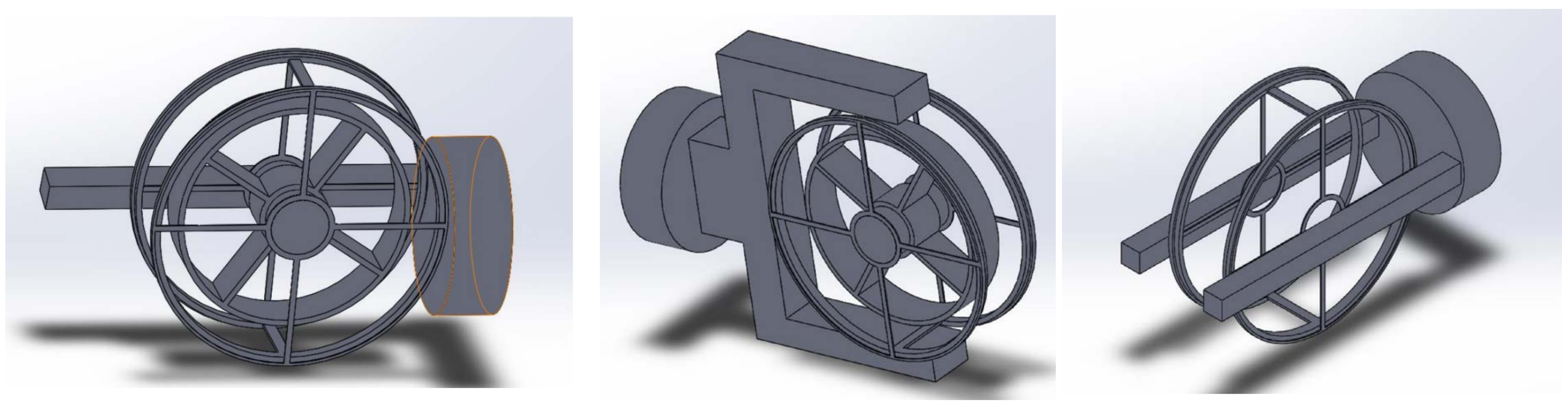

Figure 2. Conceptual designs (single-beam, yoke, and front end loading

Detailed Design Phase

Our detailed design features a simply supported beam setup, where the end of the beam opposite of the power transmitting shaft is supported by a yoke with three urethane rollers to allow for rotational movement. The center of this rotational support is aligned with the center of the power transmitting shaft to prevent any translational movement. The design also features a spring loaded locking mechanism, which is controlled from the center of the wheel and allows the operator to simply open and close the side enclosure to lock spools of tubing into place. The entire mechanism, with the exception of the base and shafts, is made from 6061-T6 aluminum, for its relatively high strength as compared to its weight as well as its welding potential as compared to other aluminum alloys.

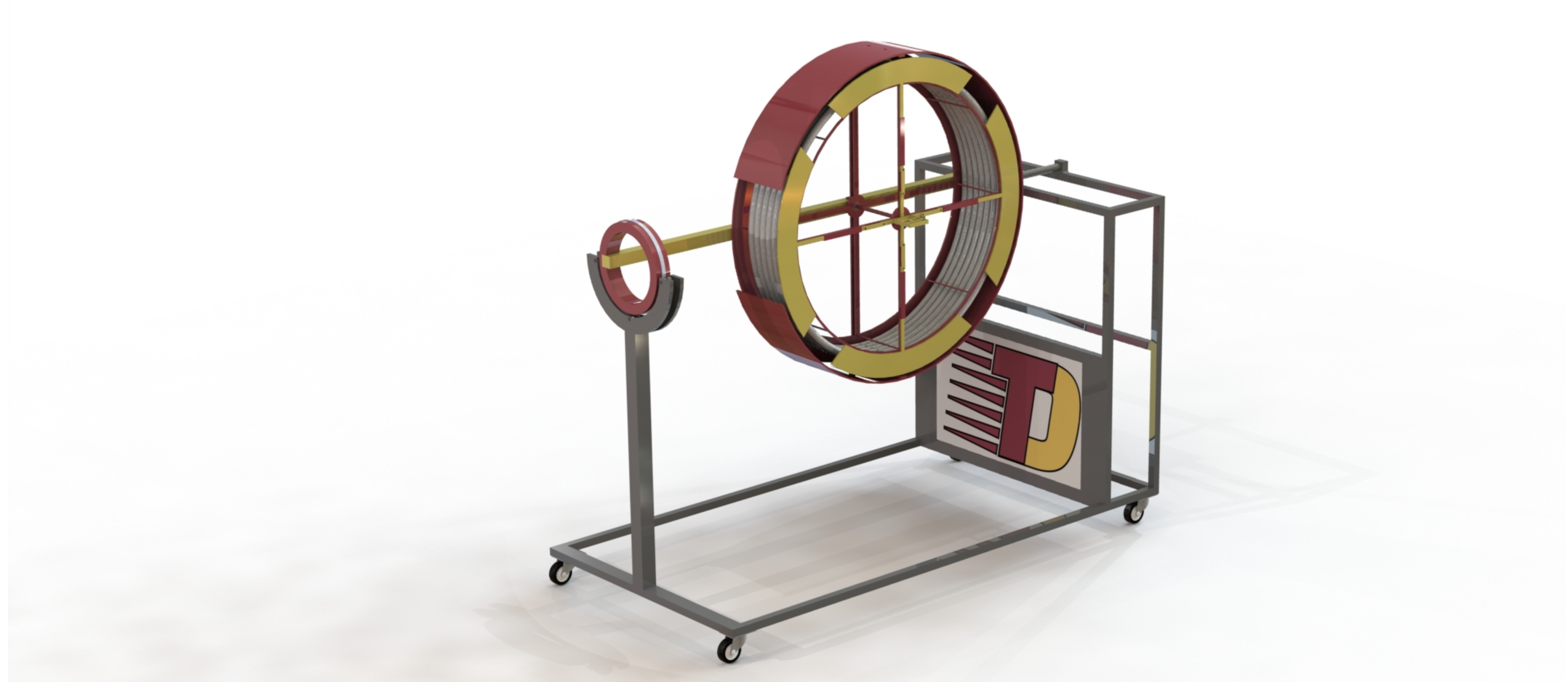

Figure 3. Rendering of current design

Prototype & Test

Structural analysis for both the large and small spindle was performed using ANSYS workbench. Our main points of concern were the deflection in the supporting beam as well as the stresses within the powered and unpowered shafts. From our simulations, all of the members operated well within the bounds of their material properties. The addition of the yoke support at the front of the spindle allowed for zero deflection at the end of the beam, allowing for the tubing to be fed into the extrusion die at approximately the same height as the die.

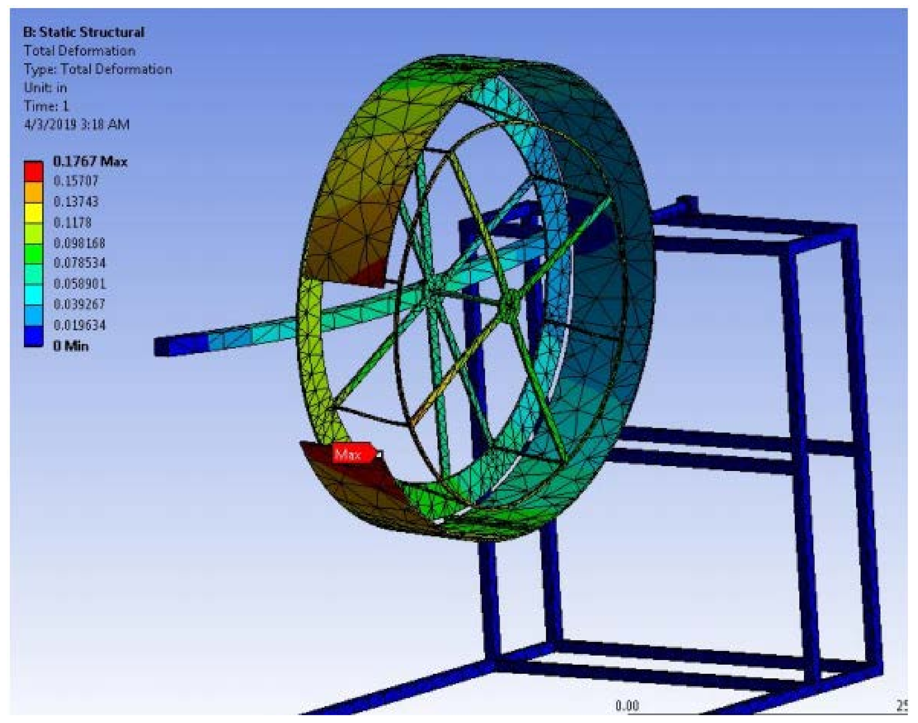

Figure 4. deflection of assembly

Conclusions

The side loading method of our spindle will drastically reduce loading time for the operator as well as eliminate the need for the staging area. By fully enclosing the tubing, the chances of the tubing slipping out of the spindle is greatly reduced, increasing safety on the manufacturing floor. From our structural analysis it was seen that the spindle is more than capable of supporting itself and the heaviest tubing used in our manufacturing process.

Originally, only two spindles were supposed to be made for Parker Hannifin-Fort Worth division. During our most recent meeting with Parker Hannifin, our client had an executive from another one of their plants join us and expressed interest in implementing our design in other manufacturing floors as well.

We would like to thank our client, Parker Hannifin for giving us the opportunity to work on this project for them as well as our faculty advisor, Dr. Raul Fernandez for providing invaluable guidance throughout the duration of our project. We would also like to thank Richard Scott, an adjunct professor here at UTA who aided us with our structural analysis and simulations.

Parker

References

1. Norton, Robert L., *Machine Design: An Integrated Approach.* 5th ed., Prentice Hall, 2014.

Carbon Fiber Monocoque

Berggren, S., Cardamone, A., Miller, J., Shead, T., Zaveri, M., Morin, J.
ME Senior Design

UNIVERSITY OF TEXAS ARLINGTON | COLLEGE OF ENGINEERING

Executive Summary

CM Engineering is producing the design and manufacturing process outline for a carbon fiber monocoque chassis for UTA's Formula SAE racecar. The goal is to produce the designs and certify that the carbon fiber chassis will be lighter, stiffer, and meet all of the safety and rule requirements for the competition. To do so physical testing has been carried out to demonstrate the stiffness and energy absorption ability of the laminates that will be used to construct the chassis.

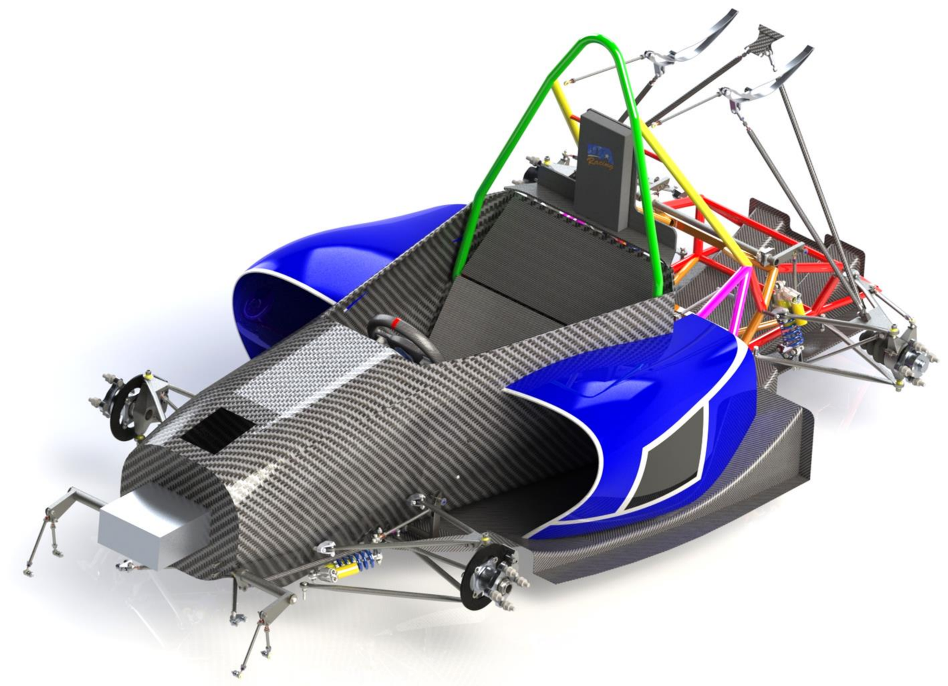

Figure 1. Monocoque Assembly

Background

Carbon monocoques were first used by McLaren in 1982 in professional racing and since then it has been a vital part of professional racing. Weight reduction is a crucial aspect of racing which drives the development of lightweight components using advanced materials such as carbon fiber. Carbon fibre alone, is very rigid but does not provide the required bending stiffness required for a chassis, thus a core material, such as aluminum honeycomb is sandwiched between the layers. This creates a lightweight structure which is very resistant loads both in and out of plane of the laminate. It is estimated that the monocoque will provide a weight reduction of 15 lbs while exceeding the performance and safety requirements.

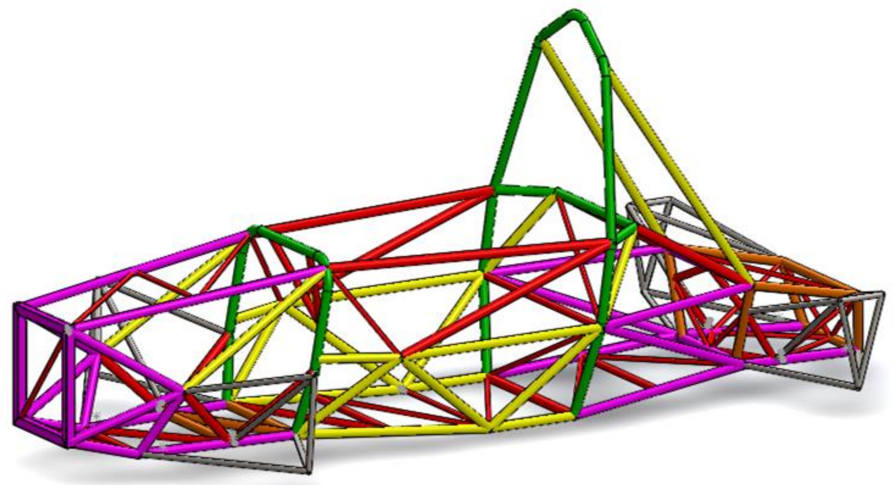

Figure 2. UTA Racing Steel Chassis

Conceptual Design Phase

A surface model of the monocoque was generated in Solidworks to allow the chassis to be shaped around the driver and mated to other components of the car such as the suspension and rear subframe. Initial FEA were run on the structure to estimate the laminate stiffness needed to satisfy performance criteria. It was concluded that 4 layers of carbon fiber on either side of a honeycomb core would be sufficient to reach the desired stiffness for the chassis. The strength requirements were determined by the FSAE rulebook and multiple test panels were created to represent the side structure which would protect the driver in a side impact. A 3 point bend test was used to determine the amount of energy the laminate could absorb before failure and multiple panels were tested to establish a trend between facesheet thickness and failure mode. The lightest panel which was able to exceed the FSAE required energy absorption was selected for the side impact structure.

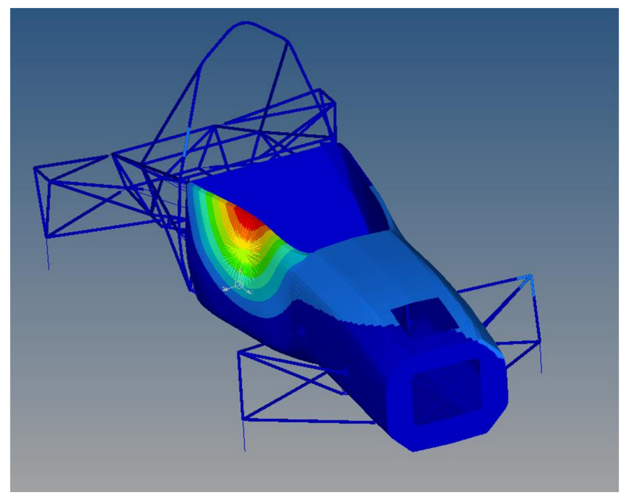

Figure 3. FEA of side impact loadcase

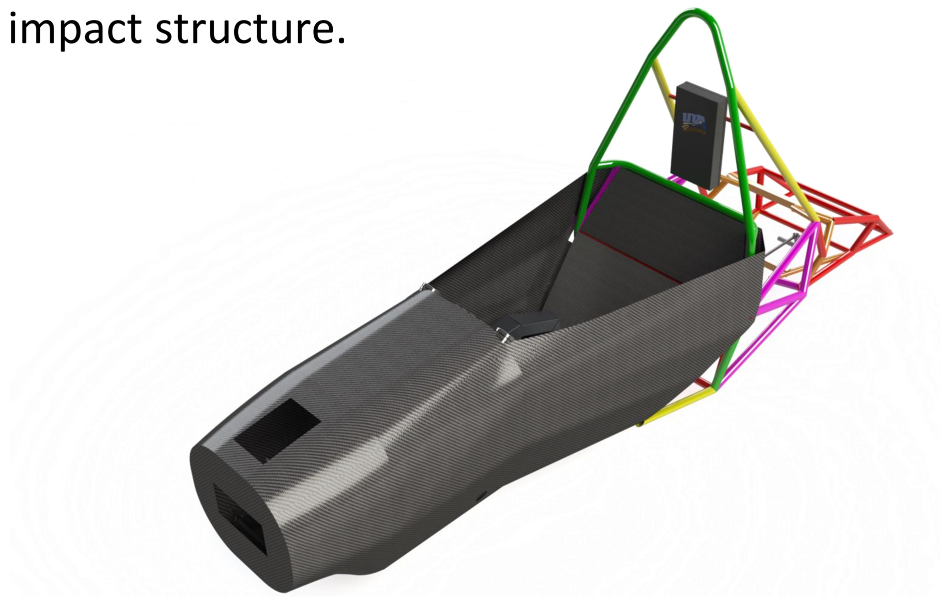

Figure 4. Initial Chassis Design

Detailed Design Phase

Different materials can be used for the core of carbon fiber sandwich panels such as nomex, foam or aluminum honeycomb. Choosing the core material came down to manufacturing constraints, and testing requirements. Aluminum honeycomb was selected because of its low density and high shear and compressive strength. The number of plys on each face sheet was determined by running a series of physical tests on panels with different construction. Since the chassis is responsible for integrating the various systems of the car, various fastening methods are examined. There are a few different fastening techniques such as potted inserts and through bolts. Potted inserts will be used for fastening items with smaller loads while higher load fasteners such as suspension clevis will use through bolts. Unlike a traditional monocoque this design only utilizes a carbon fiber sandwich panel structure for the drivers cell while the region behind the driver will still be a steel space frame. FSAE rules have major changes every 2 years and by maintaining a steel rear structure the chassis has flexibility to mount different engines without needing to machine new molds.

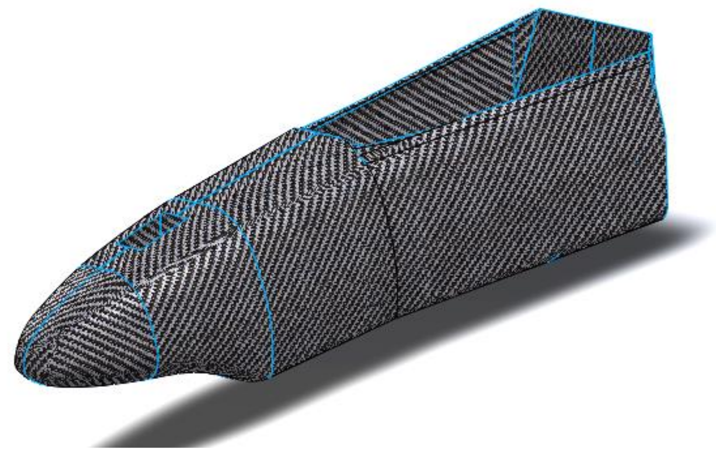

Figure 5. Monocoque Chassis

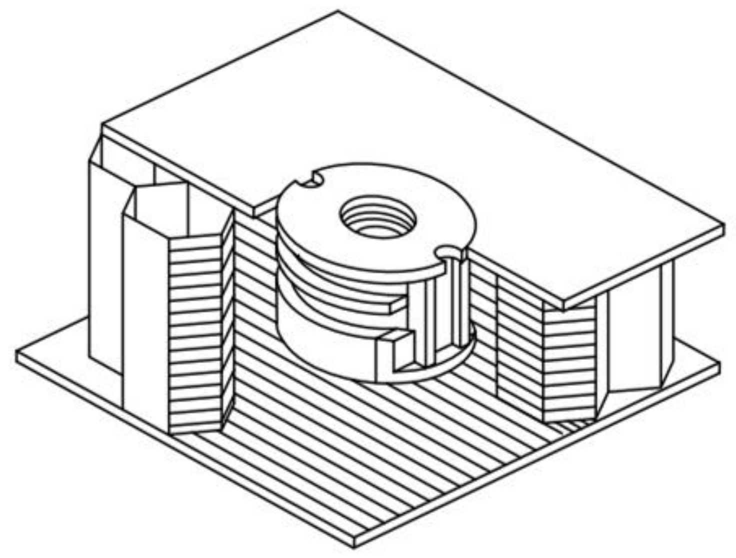

Figure 6. Potted Insert

Prototype & Test

The physical testing performed was a perimeter shear test and a 3-point bend test to check conformity with FSAE rules. The perimeter shear test involved punching a 25mm hole into a 100mm x 100mm test specimen. The specimen must withstand 4kN to be compliant for the front of the chassis while 7.5kN is required for the side impact structure. The 3-point bend test is only required for the side impact structure and must absorb the same amount of energy as 2, 1inch x 0.065inch tubes. Each test specimen 275mm x 500mm and support a span of 400mm. The test results concluded that a symmetric layup of 4 plies per face sheet with ⅜inch aluminum honeycomb was sufficient for the front of the chassis while 8 plies on the compression side and 4 plies on the tension side was required for the side impact structure.

Figure 7. Perimeter Shear Test

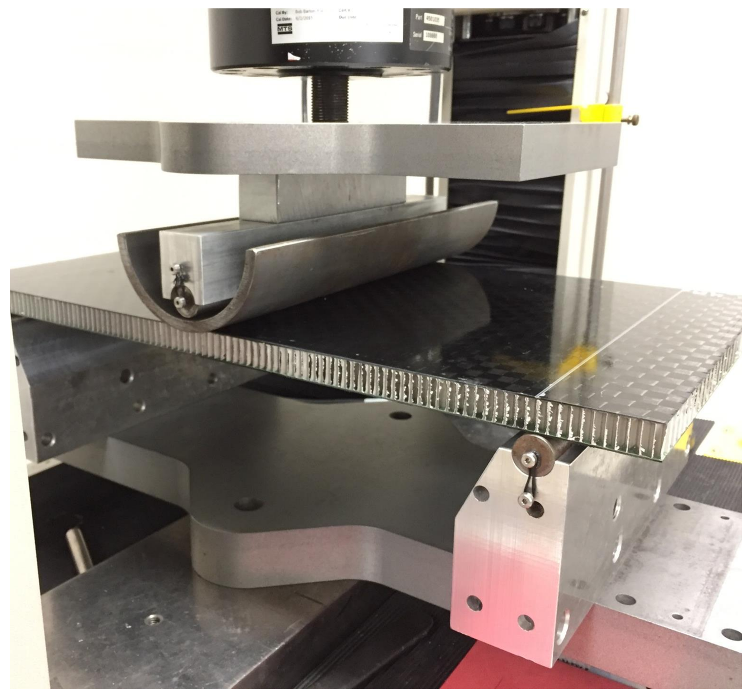

Figure 8. 3-Point Bend Test

Conclusions

The monocoque design created by our team was able to reduce the weight of the chassis while maintaining a high level of performance and safety. Physical testing provided crucial insights on the number of layers of carbon and the type of aluminum core to be used. FEA of the laminate concluded that 5/8in aluminum honeycomb would yield the required stiffness with 4 plies on either side for the front section of the monocoque. However, the side impact structure would comprised of the same core but with 4 plies on the tension side and 8 plies on the compression side. While the initial FEA was able to accurately predict the stiffness of the laminate, physical testing was key in determining the strength and failure mode of the laminate. Future plans are to finalize tooling method for the monocoque tooling and provide a full detailed manual of the manufacturing process to the UTA Racing Team. This manual will serve as a step by step guideline so that the team can implement our design in UTA's 2020 racecar. CM Engineering would like to thank the UTA Racing Team, Dr. Robert L. Woods for their immense support, guidance and equipment use.

References

J. R. VINSON. "Optimum design of composite honeycomb sandwich panels subjected to uniaxial compression", AIAA Journal, Vol. 24, No. 10 (1986), pp. 1690-1696.
https://doi.org/10.2514/3.9502
Steeves, C. A., & Fleck, N. A. (2004). Collapse mechanisms of sandwich beams with composite faces and a foam core, loaded in three-point bending. Part I: Analytical models and minimum weight design. International Journal of Mechanical Sciences, 46(4), 561-583. doi:10.1016/j.ijmecsci.2004.04.003

2019 UTA College of Engineering Innovation Day April 15, 2019

Wheelchair Dynamometer

UNIVERSITY OF TEXAS ARLINGTON | COLLEGE OF ENGINEERING

Griffin, B., Araujo, A., McCormick, M., Goodlow, C., Gulledge, J., Niestroy, M.
ME Senior Design

Executive Summary

The purpose behind the wheelchair dynamometer is to assist the UTA Department of Kinesiology and UTA Movin' Mavs with data acquisition and means for wheelchair users to exercise.

The team built from a legacy design. After analyzing the design, the team had a few concerns to address: safety, manufacturability, and ergonomics.

Since operator safety is paramount, the team developed retention features on the ramps and rollers in order to prevent users from falling off. A few manufacturability concerns arose throughout the duration of the project. Previous fabrication attempts led to distortion in key areas of the frame which required follow-on corrections. Several components were modified to improve the user experience while operating the dynamometer.

The Wheelchair Dynamometer team has completed the intended deliverables, which include a full mechanical system and technical data package, while operating ahead of schedule and below budget.

Background

The Movin' Mavs basketball team submitted a request for a wheelchair dynamometer, seen in Figure 1, in 1993. The request has since been resubmitted as they desired a dynamometer that matches the quality of modern fitness equipment. The ultimate goals were to fulfill the athletes' need to train and enhance the biomechanicist's research data acquisition process.

This system was intended to be simple to use and avoid the requirement that the wheelchair be restrained (as seen in traditional dynamometers). Electric motors were requested to provide variable resistance alongside a flywheel system to prevent overexertion.

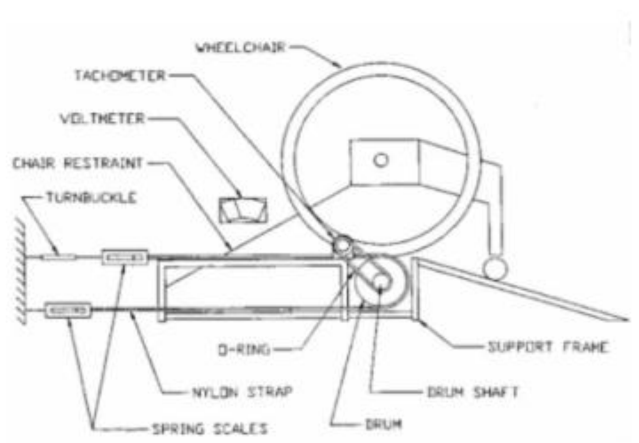

Figure 1. Design from 1993

Conceptual Design Phase

The legacy design inherited from the previous team required verification of key dimensions and features. An example of a key dimension that was verified and modified is the spacing of the front and rear roller assemblies as seen in Figure 2. The spacing of the rollers is instrumental in allowing the operator to exert maximum force without inadvertently exiting the system.

Figure 3 displays an early conceptual design for the flywheel attachment method. While the system later adopted a keyed method to transmit the torque, the early design implemented a more complex method of attachment.

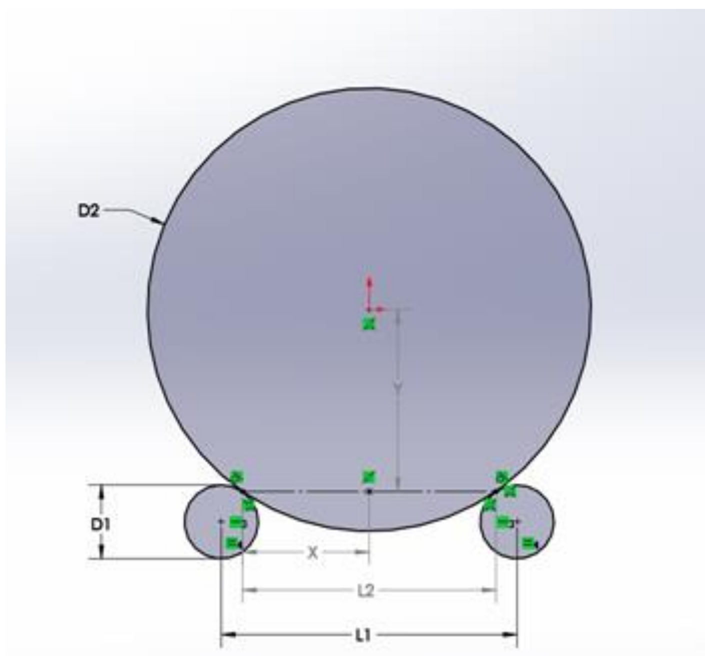

Figure 2. Force to Escape

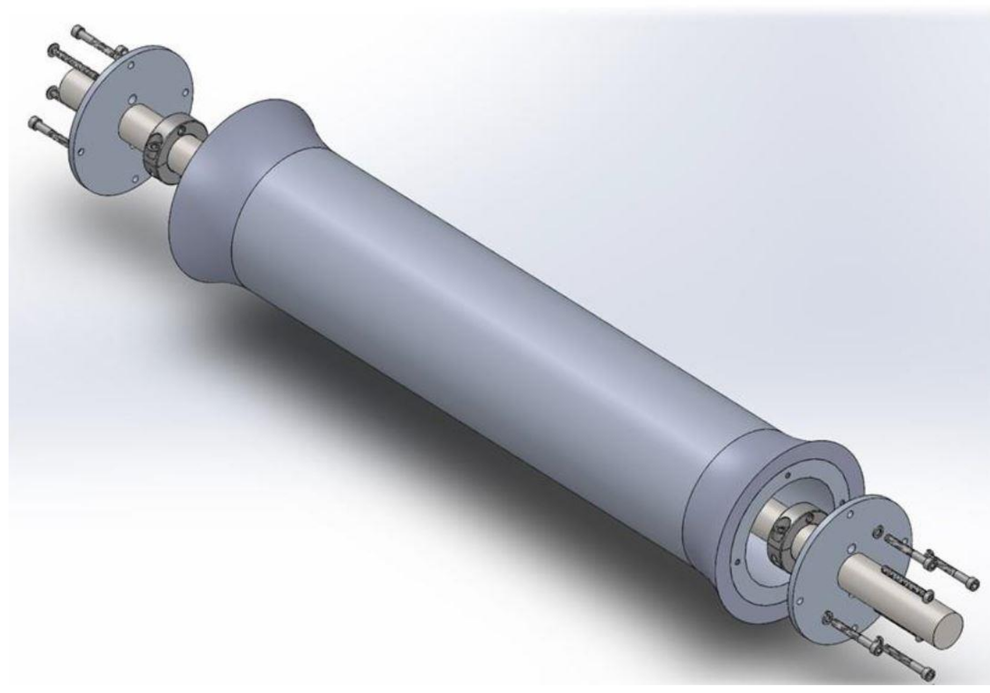

Figure 3. Early Flywheel Concept

Detailed Design Phase

The team's primary focus was to design the system in SolidWorks for seven weeks and begin manufacturing immediately after. This included extensive tolerancing on key features such as the rollers, the flywheel, and the brake/lift mechanism since these have a direct impact on the experience of the user. This became a balance of designing for manufacturing/assembly, and reducing the burden on the machine shop by only tightening tolerances where required. For example, the solution implemented for the rollers in order to remain concentric with the axis of rotation was to use shoulder bolts to locate the position of the coupler relative to the shaft. This allows for easy assembly, but provides a robust solution to ensure design intent is carried out.

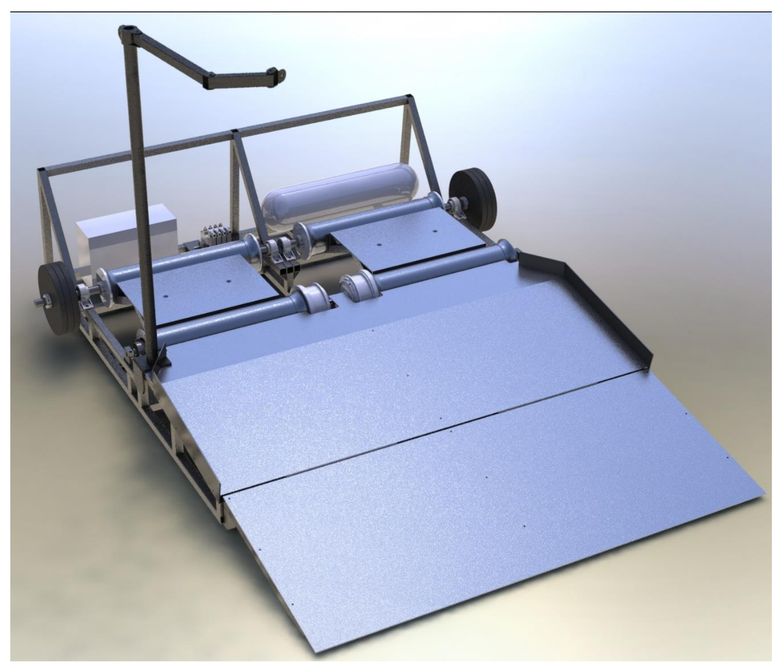

Figure 4. Fully Rendered Model

Figure 5. Final Assembly

Prototype & Test

The team conducted internal tests to confirm the functionality of the pneumatic system before installing them on the platform. Additionally, testing was necessary to determine the validity of using spray adhesive to affix the rubber to the aluminum. Ultimately, rivets replaced the adhesive due to its poor performance. Prior to powder coating, the system was fully assembled to ensure correct fit. Upon assembly, it was determined that the inner diameter of the flywheel mechanism had excess clearance and required bushings to be machined and brazed to the plates.

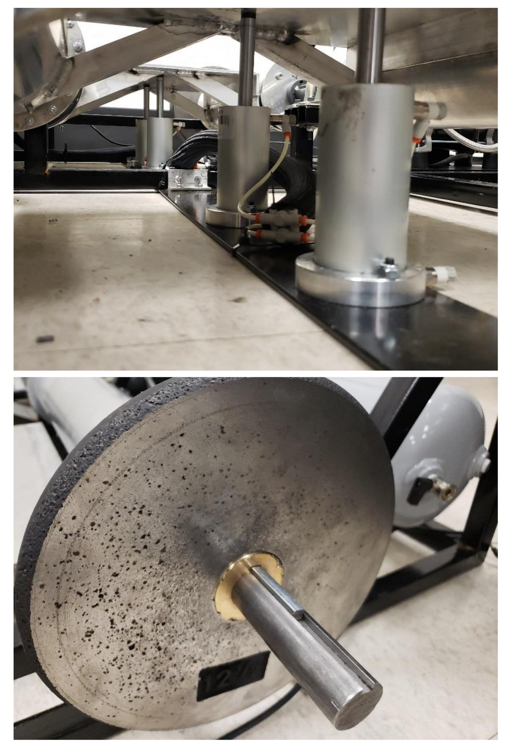

Figure 6-7. Pneumatics [top] Flywheel [bottom]

Figure 8. Mid-Production Prototype

Conclusions

As the team approaches the end of this project, it is apparent that the system satisfies the goals and expectations of our faculty advisor, Dr. Woods, and our client, Mr. Garner. In order to satisfy the planned capabilities promised to the client, the system awaits the integration with the electrical engineering team. There were many lessons learned regarding design for manufacturing and proper tolerancing for the key components. Once the dynamometer is fully integrated, it will replace the treadmill currently with the kinesiology department. We would like to thank Dr. Woods and Michael Baldwin from SMC for their time and donations.

References

1. Dynomatic Engineering & Innovations' Final Project. University of Texas at Arlington, 2017
2. Diaz & Company's Final Project. University of Texas at Arlington 2018